Title

Autonomic and respiratory components of orienting behaviors are mediated by descending pathways originating from the superior colliculus

Authors

Erin Lynch[1], Bowen Dempsey[2], Eloise Monteiro[1], Anita Turner[1], Christine Saleeba[1], Peter GR Burke[1], Andrew M Allen[3], Roger AL Dampney[4], Cara M Hildreth[1], Jennifer L Cornish[1], Ann K Goodchild[1] & Simon McMullan*[1]

Affiliations

1. Faculty of Medicine, Health & Human Sciences, Macquarie University, NSW 2109 AUSTRALIA
2. Institut de Biologie de l'ENS (IBENS), Inserm, CNRS, École normale supérieure, PSL Research University, Paris, FRANCE.
3. Department of Anatomy and Physiology, University of Melbourne, Victoria, 3010 AUSTRALIA
4. School of Medical Sciences (Physiology), University of Sydney, NSW 2006, AUSTRALIA

Contact Info

Correspondence: Simon McMullan, simon.mcmullan@mq.edu.au

Summary (150 words)

The ability to discriminate competing, external stimuli, and initiate contextually appropriate behaviors, is a key brain function. Neurons in the deep superior colliculus (dSC) integrate multisensory inputs and activate descending projections to premotor pathways responsible for orienting and attention, which often involve adjustments to respiratory and cardiovascular parameters. However, the neural pathways that subserve physiological components of orienting are poorly understood. We report that orienting responses to optogenetic dSC stimulation are accompanied by short-latency autonomic, respiratory and electroencephalographic effects in conscious rats, closely mimicking those evoked by naturalistic alerting stimuli. Physiological responses were not accompanied by detectable aversion or fear and persisted under urethane anesthesia, indicating independence from emotional stress. Moreover, autonomic responses were replicated by selective stimulation of dSC inputs to a subregion in the ventromedial medulla containing spinally-projecting premotor neurons. This putative disynaptic pathway from the dSC represents a likely substrate for autonomic components of orienting.

Introduction

The neural networks that control the circulatory and respiratory systems are co-opted by intrinsic and extrinsic stressors such as pain, fear and anger. Known widely as ‘defense’ or ‘fight-or-flight’ responses, this context-specific co-activation of cardiovascular, respiratory and behavioral states corresponds, in humans, with the conscious perception of emotion (Dampney et al., 2008; Kataoka et al., 2020; Silva et al., 2016). However, *defensive behaviors* are preceded in all vertebrates by *orienting responses*, the initial component of a pattern of activity that can transition to behaviors such as escape from a predator or pursuit of a prey, depending on the precise nature of the stimulus (Krauzlis et al., 2018).

In this context, novel, often innocuous, salient environmental stimuli that drive orienting responses also generate pronounced transient cardiovascular and respiratory effects. For example, unexpected sounds produce increases in arterial pressure (Baudrie et al., 1997; Caraffa-Braga et al., 1973; Rettig et al., 1986; Yu and Blessing, 1997), mesenteric and cutaneous vasoconstriction (Caraffa-Braga et al., 1973; Yu and Blessing, 1997), and increases in respiratory rate (Kabir et al., 2010; Nalivaiko et al., 2012), with little change in heart rate (Baudrie et al., 1997; Kabir et al., 2010; Nalivaiko et al., 2012). Visual or somatosensory stimuli can also evoke similar cardiovascular and respiratory responses (Kabir et al., 2010; Yu and Blessing, 1997). These effects are also typically accompanied by cortical electroencephalographic (EEG) desynchronization, superimposed by a prominent hippocampal theta rhythm (5-8 Hz) (Nalivaiko et al., 2012; Yu and Blessing, 1997), an electrophysiological signature of orientating, attention, and navigational behaviors, widely interpreted as an index of engagement with the environment (Buzsáki, 2006).

The superior colliculus (SC) is a phylogenetically conserved brain region that plays a critical role in generating innate behavioral responses, including orienting, to salient environmental stimuli (Isa et al., 2020; Sparks et al., 1990). Its deeper layers (dSC) receive convergent inputs from visual, auditory and somatosensory receptors, as well as from other brain regions including the basal ganglia and frontal and parietal cortices, and provide direct descending projections to motor and premotor nuclei in the brain stem and spinal cord that mediate behavioral responses (Boehnke and Munoz, 2008; Dean et al., 1989; May, 2006; Meredith and Stein, 1986). Under anesthesia, electrical or chemical stimulation of sites within the dSC evokes increases in arterial pressure, respiratory activity and sympathetic vasomotor nerve activity (Iigaya et al., 2012; Keay et al., 1990; Keay et al., 1988), whereas, dSC disinhibition augments sympathetic and respiratory responses to brief auditory, visual and somatosensory stimuli (Müller-Ribeiro et al., 2014; Müller-Ribeiro et al., 2016). Collectively, these observations suggest that, although normally subject to tonic inhibitory control, neurons in the dSC have the capacity to generate behavioral motor responses to alerting environmental cues and may also trigger autonomic and respiratory changes that support motor responses. However, the central pathways that underlie respiratory and autonomic components of dSC-mediated responses, and the behavioral contexts in which they are activated, are unclear.

Here we investigate the hypothesis that dSC neurons drive autonomic and respiratory adjustments independent of the pillars of the classic defense response: cortical processing, emotion and psychological stress. Using optogenetic stimulation in conscious rats, we show that dSC stimulation evokes orienting behaviors that are accompanied by short-latency autonomic, respiratory and EEG effects that closely mimic responses evoked by naturalistic alerting stimuli. We show that these responses occur in the absence of detectable aversion or fear responses, indicating that they are not part of the defense response, and that such autonomic and respiratory effects are maintained under anesthesia and driven by a descending pathway that includes a relay in the ventromedial medulla oblongata.

Results

dSC stimulation drives alerting, orienting, and physiological responses in behaving rats

Experiments focused on a region of the rat caudolateral dSC (cl-dSC: Figure 1) which, when disinhibited, unmasks respiratory, cardiovascular and somatomotor responses to visual and auditory stimuli under urethane anesthesia (Müller-Ribeiro et al., 2014; Müller-Ribeiro et al., 2016). Following viral transduction of this region to express Channelrhodopsin2 (ChR2), optogenetic stimulation (63 – 160 mW/mm^2, 5-10 Hz, 20 ms pulses, 5-10 s) evoked stimulus-dependent orienting responses in conscious rats, first detectable as a pause in ongoing behavior with contraversive head-turning (Figure 1A). This response was not seen in animals injected with a control, non-ChR2-expressing vector. As stimulus intensities increased, head-turning became more pronounced and sometimes led to transient full-body turning (Figure 1A, Video 1). At the highest stimulus intensities tested (320 mW/mm^2, 10-20 Hz, 20 ms pulses, 5-10 s) the initial pause and head-turning component of the response was often bypassed, and instead rats transitioned into full-body turning, consistent with recent reports in the mouse and rat (Isa et al., 2020; Soper et al., 2016). Co-ordinated locomotor responses, such as running, were rare, and clear defensive behaviors, such as freezing, explosive escape or retreat, typical of stimulation of the rostromedial tectal defense pathway (Isa et al., 2020), were only seen in 1/33 rats.

At the conclusion of cl-dSC activation, motor effects abruptly ceased and rats reverted to their previous behaviors without discernable signs of fear or heightened vigilance, such as aversion to approach or handling. To more closely assess whether stimulation of the cl-dSC elicited anxiety-like behaviors that outlasted stimulus presentation, we adapted the stimulus protocol (320 mW/mm^2, 1 Hz, 20 ms pulses, 1-2 min: Figure 1B), after which rats were immediately transferred onto either an open field or an elevated plus maze apparatus. Under these conditions cl-dSC stimulation was not associated with detectable changes in open field (ChR2 vs. control vectors, unpaired t-test, $P = 0.6$) or plus maze exploration (unpaired t-test, $P > 0.99$, Figure 1C). Similarly, activation of the cl-dSC was not associated with low- or high-frequency ultrasonic vocalizations, indices of aversive and appetitive stimuli, respectively (Brudzynski, 2007; Brudzynski, 2013), during stimulation in the home cage (unpaired t-test, $P = 0.2$) or exploration of the plus maze (unpaired $P = 0.9$, Figure 1D). On the other hand, 1 Hz cl-dSC stimulation continued to evoke orienting and motor effects, quantified as an increase in circling and distance travelled during stimulation, measured by overhead video tracking of the nose, without exerting measurable effects on cage exploration in the post-stimulation period (Figure 2). We conclude that optogenetic cl-dSC stimulation evokes acute, transient, orienting responses and stereotypic motor activity, but that these are not associated with anxiety-like behaviors.

Much like behavioral responses to naturalistic salient stimuli (Nalivaiko et al., 2012), orienting responses evoked by cl-dSC stimulation were accompanied by profound transient elevations in respiratory rate and EEG desynchronization together with increased theta power (5-8 Hz), even at stimulation intensities that evoked minimal motor effects (63 – 160 mW/mm^2, 5-10 Hz, 20 ms pulses, 10 s, head turning only, Figure 3A). In the rat, orienting responses to innocuous naturalistic stimuli are associated with transient tail vasoconstriction (de Menezes et al., 2009; Nalivaiko et al., 2012), resulting in tail cooling and core heat retention. Infrared tail thermography revealed similar effects in response to cl-dSC stimulation (320 mW/mm^2, 1 Hz, 20 ms pulses, 10 min): tail temperature dropped to a nadir of -2.0 ± 0.4 ^{o}C during photostimulation and then rebounded to a peak of +1.1 ± 0.4^{o}C relative to baseline over the ten minutes after stimulation (RM 2-way ANOVA interaction $P < 0.0001$, Figure 3B). Activation of respiratory and autonomic outputs is therefore an inherent component of orienting responses evoked by cl-dSC stimulation.

Physiological responses to cl-dSC stimulation are maintained under anesthesia

Adjustments to blood pressure, sympathetic nerve activity and breathing are integral features of motor behaviors that result from both peripheral sensory signals and feedforward from hypothalamic central command circuits (reviewed by Dampney et al., 2008). To differentiate physiological responses evoked by cl-dSC stimulation from those dependent on motor components of orienting responses, recordings of respiratory, blood pressure, heart rate and postganglionic splanchnic nerve responses to cl-dSC stimulation were made in urethane-anesthetized rats (Figure 4). Low-frequency stimulation (320 mW/mm^2, 0.5 Hz, 20 ms pulses, 200–600 repeats) revealed constant-latency sympathoexcitatory responses in 8/11 cases (onset 43 ± 3 ms, peak 101 ± 3 ms, Figure 4D). In most experiments where sympathetic responses were observed, intensity-dependent respiratory and cardiovascular responses to short trains of repetitive cl-dSC stimulation were also observed (320 mW/mm^2, 10-20 Hz, 20 ms pulses, 10 s). Responses were characterized by abrupt increases in respiratory frequency and respiratory burst size (Figure 4C, 8/8 cases), increased mean sympathetic nerve activity (SNA, Figure 4E, 6/8 cases), and systolic arterial blood pressure (sAP, Figure 4F, 7/8 cases), with variable effects on heart rate (Figure 4G).

Physiological responses to cl-dSC stimulation are mediated via relay in the medullary reticular formation

The short latency of sympathetic responses to cl-dSC stimulation, and our previous observation that cl-dSC-facilitated autonomic responses to sensory stimulation persist following pre-collicular decerebration (Müller-Ribeiro et al., 2014), suggest a direct descending neural pathway from the cl-dSC that does not involve ascending loops through forebrain limbic or hypothalamic defense regions. Using anterograde tract tracing, we identified putative connections between cl-dSC output neurons and hindbrain autonomic and respiratory relays. Microinjection of AAV-CBA-tdTomato into the cl-dSC revealed a clearly defined ascending projection to the thalamus and hypothalamus, a projection to the contralateral superior and inferior colliculi, via the commissural nucleus of the inferior colliculus, and a descending projection to the brainstem (Figure 5S1). Confocal imaging of tdTomato-labelled hindbrain terminal fields identified close appositions in candidate autonomic nuclei (Figure 5S2), including moderate innervation of catecholaminergic neurons in the A5, A6 (locus coeruleus) and A7 (parabrachial/Kölliker-Fuse) regions. A more conspicuous and largely ipsilateral nexus of fibers and arborized varicosities extended across subnuclei within the ventromedial medulla to encompass the gigantocellular alpha (GiA) and paragigantocellular reticular nuclei and obscurus, pallidus, and magnus raphé nuclei (Figure 5A & B).

Spinally projecting neurons in this region, including V2a neurons that express the transcription factor CHX10, are considered key players in the initiation and arrest of locomotion and orienting behaviors (Dougherty and Kiehn, 2010; Usseglio et al., 2020), and were confirmed recipients of putative inputs from labelled cl-dSC neurons (Figures 5C, 5S2). However, this region of the rostral ventromedial medulla is also a major site of sympathetic premotor neurons that innervate vasomotor and non-vasomotor targets (reviewed by Dampney, 1994; Stornetta, 2009), and its neurochemically diverse constituents are also implicated in respiratory and somatosensory functions (Crone et al., 2012; Depuy et al., 2011; Morris et al., 1996; Porreca et al., 2002). To test whether, in addition to a postulated role in coordinating motor effects of dSC stimulation (Isa et al., 2020), activation of this pathway contributes to the physiological effects evoked by cl-dSC stimulation, we injected AAV-Syn-ChR2-YFP in the cl-dSC and optically stimulated ChR2-transduced axon terminals in the GiA in urethane-anesthetized rats. Expression of ChR2-YFP in the ipsilateral GiA was always present in rats where photostimulation drove physiological responses (Figure 6). The profiles of sympathetic (Figure 6C) and pressor

(Figure 6D) responses to 20 Hz GiA stimulation were not significantly different from those evoked by 20 Hz cl-dSC stimulation (2-way ANOVA interaction P>0.99 for both sympathetic and pressor responses, n = 7, direct comparison in Figure 6S1A). Although GiA stimulation increased respiratory frequency in 4/7 cases, effects were consistently smaller than those evoked by cl-dSC stimulation (10 ± 3 vs. 29 ± 7%, unpaired t-test P = 0.036, Figure 6S1B). In 4/5 animals tested, low-frequency GiA stimulation (320 mW/mm^2, 0.5 Hz, 20 ms pulses) evoked sympathoexcitatory responses that occurred at a shorter latency (onset 30 ± 1 vs. 43 ± 3 ms, unpaired t-test P = 0.02) but equivalent peak amplitude (151 ± 14 vs. 163 ± 25%, unpaired t-test P = 0.76) compared to cl-dSC stimulation (Figure 6E).

Extracellular recordings confirmed that sympathetic responses to GiA stimulation are likely mediated via direct activation of local sympathetic premotor neurons (Figure 7). In two urethane-anesthetized rats, 7/7 spontaneously active (12.6 ± 5.1 Hz) spinally-projecting GiA neurons (spinal conduction velocity 12.5 ± 2.8 m/s) exhibited frequency-dependent excitatory responses to cl-dSC stimulation (320 mW/mm^2, 20 ms pulses: 10 Hz: +28 ± 9%; 20 Hz: +72 ± 14%, Figure 7C), and low frequency cl-dSC stimulation (320 mW/mm^2, 0.5 Hz, 20 ms pulses) revealed short latency excitatory responses in 2/4 cells tested (8, 17 ms Figure 7D). Several units (4/7) were identified as putative sympathetic premotor neurons based on entrainment of unit discharge to blood pressure pulsatility (n = 3, Fig 7E) or covariation of neuronal discharge with SNA, revealed by spike-triggered averaging (n = 4, data not shown).

Discussion

Here we show that, in freely behaving rats, stimulation of the cl-dSC at intensities that drive orienting responses, EEG desynchronization and theta rhythm, evokes transient respiratory and cutaneous vasomotor responses that are consistent with the effects evoked by natural salient stimuli (de Menezes et al., 2009; Nalivaiko et al., 2012; Yu and Blessing, 1997). The brief nature of responses and the absence of anxiety-like or avoidant behaviors differentiates them from autonomic and respiratory responses evoked by psychological stress, which outlast stimulus presentation (Ootsuka et al., 2017; Vianna et al., 2008; Vianna and Carrive, 2005), and suggests independence from the canonical defense response.

Detailed physiological recordings under anesthesia recapitulated the respiratory effects seen in behaving animals and revealed excitatory effects on SNA, which were similar in latency to those evoked by direct stimulation of sympathetic premotor neurons (Abbott et al., 2009; Menuet et al., 2014). Stimulation of the cl-dSC also evoked pressor effects with little change in heart rate, mimicking the pattern of cardiovascular effects recruited by alerting stimuli, thought to result from activation of vasomotor sympathetic nerves and co-activation of cardiac sympathetic and parasympathetic nerves (Casto and Printz, 1990; Nalivaiko et al., 2012). Viral anterograde tracing of cl-dSC neurons defined two main descending pathways, a major ventral pathway to the ventromedial medulla and a minor dorsal pathway that targeted the dorsomedial spinal trigeminal nucleus. Stimulation of cl-dSC efferent terminals in the GiA region of the ventromedial medulla mimicked the autonomic pattern evoked by direct stimulation of the cl-dSC. Interestingly, the respiratory response to stimulation of dSC-GiA axons was reduced compared to direct stimulation of the cl-dSC, indicating that involvement of a separate supplementary respiratory circuit might be required for full elaboration of respiratory effects. Spinally projecting autonomic neurons in the same area were functionally identified *in vivo* by their transmission of cardiovascular information (Chen and Toney, 2010; McMullan et al., 2007; Morrison et al., 1988; Turner et al., 2013), and shown to receive excitatory input from the cl-dSC.

Previous studies reported that autonomic responses to visual, acoustic and somatosensory stimuli, unmasked by disinhibition of the cl-dSC, persist following pre-collicular decerebration (Müller-Ribeiro et al., 2014). We reasoned that the physiological effects of dSC stimulation may reflect a previously unrecognized descending pathway, and used anterograde tracing to identify putative relays to medullary respiratory and autonomic nuclei. We observed no anatomical evidence of innervation of the rostral ventrolateral medulla (RVLM) by cl-dSC output neurons. This is perhaps surprising, as RVLM neurons are: a major source of excitatory drive to sympathetic nerves and play a critical role in subserving a wide range of cardiovascular reflexes (Dampney, 1994; Guyenet, 2006); implicated in mediating sympathetic responses to a range of physiological and psychological stressors (Abe et al., 2017; Guyenet et al., 2013; Zhao et al., 2017); and reported to receive monosynaptic input from the SC (Dempsey et al., 2017; Stornetta et al., 2015). In contrast, we found extensive arborization of cl-dSC efferents across multiple mRF compartments, most prominently the GiA, which is a major hub for descending control to spinal locomotor circuits (Bouvier et al., 2015; Dougherty and Kiehn, 2010; Kim et al., 2017; Perreault and Giorgi, 2019; Usseglio et al., 2020). Similar SC innervation of the mRF has been described previously in the mouse and rat (Isa et al., 2020; Redgrave et al., 1987; Usseglio et al., 2020). GiA neurons are potently stimulated by alerting stimuli (Furlong et al., 2014) and are implicated in mediating motor responses to SC stimulation (Isa and Sasaki, 2002). However, in addition to its motor functions, the GiA and lateral paragigantocellular nucleus contain abundant sympathetic premotor neurons that innervate brown adipose, visceral and cutaneous targets (Cano et al., 2001; Card et al., 2011; Morrison, 1999; Rathner and McAllen, 1999; Standish et al., 1995; Strack et al.,

1989; Varner et al., 1992), making this region uniquely suited for integration of motor and autonomic commands from the SC.

Optogenetic stimulation of cl-dSC-GiA terminals evoked pressor and sympathetic effects equivalent to those elicited by cl-dSC activation, with sympathoexcitatory responses to single-pulse GiA stimulation occurring at shorter latencies than those evoked by cl-dSC stimulation. Extracellular recordings from functionally identified GiA sympathetic premotor neurons confirmed excitatory responses to cl-dSC stimulation at a latency (~10 ms) that aligns well with the difference between sympathoexcitatory responses evoked by single-pulse cl-dSC vs. GiA stimulation (~13 ms). Taken together, these findings suggest that sympathetic responses to cl-dSC stimulation are principally due to activation of GiA neurons and confirm a role for bulbospinal sympathetic premotor GiA neurons. Based on the latency of responses and the results of our anterograde tracing experiments, this pathway is likely disynaptic and unlikely to involve supramedullary sites.

In contrast, respiratory responses to cl-dSC-GiA terminal stimulation were consistently smaller than those evoked by direct cl-dSC stimulation, suggesting the necessary involvement of neurons within and beyond the GiA for full respiratory effects. Potential local mediators of respiratory responses include serotonergic raphe obscurus neurons and non-serotonergic GiA neurons, stimulation of which evokes tachypnoea (Depuy et al., 2011; Verner et al., 2004). Supramedullary contributors to cl-dSC-evoked tachypnoea could include the parabrachial/Kölliker-Fuse complex and periaqueductal grey, stimulation of which increases respiratory rate under anesthesia (Chamberlin and Saper, 1994; Hayward et al., 2003) and both of which were identified as sites of dSC terminal fields in the current study.

The present study identifies a novel pathway that links neurons in the SC with autonomic and respiratory actuators in the medulla, but two key questions remain. First, do cl-dSC projections target separate populations of GiA neurons that drive distinct descending motor and autonomic pathways, or do they target multifunctional GiA neurons that provide divergent excitatory drive to respiratory, sympathetic and somatic motor pools? The latter seems possible: genetic deletion of V2a neurons, the quintessential reticulospinal premotor cell group and a major dSC target (Dougherty and Kiehn, 2010; Usseglio et al., 2020), is associated with motor deficits (Crone et al., 2008; Crone et al., 2009) and a severe hypoventilation phenotype that persists in the isolated medullary slice (and therefore not attributable to spinal V2a depletion: Crone et al., 2012). Similarly, polysynaptic viral tracing indicates that at least 20% of GiA bulbospinal neurons provide dual innervation to motor and autonomic targets (Kerman, 2008). These findings are consistent with an emerging view of mRF neurons as containing distinct functionally diverse subpopulations (Usseglio et al., 2020), which could make them well-placed to orchestrate adaptive motor, respiratory and autonomic responses to salient environmental cues.

The second question regards the behavioral contexts under which this pathway is activated. The superior colliculus is a critical node for the selection and execution of innate behavioral responses to multimodal environmental cues (Saidel, 2009; Yilmaz and Meister, 2013). Its structure is highly conserved across vertebrate groups (Butler and Hodos, 2005), and organized to reflect the topography of the sensory inputs that converge upon it (Stein and Meredith, 1993). As a consequence, different regions of the SC process inputs that vary not only in their somatotopy, but also in their ecological saliency (Comoli et al., 2012), and correspondingly evoke distinct patterns of motor activity, including orienting, predation, avoidance and escape (Basso and May, 2017; Furigo et al., 2010; Shang et al., 2019; Sparks et al., 1990; Yilmaz and Meister, 2013). Our experiments confirm a recent report by Isa et al. (2020), which describes intensity-encoded orienting in response to optogenetic activation of the analogous region of the mouse caudolateral dSC, and

contrast with the escape and freezing behaviors evoked by stimulation of the rostromedial dSC (Sahibzada et al., 1986; Wei et al., 2015). Whether the cl-dSC pre-autonomic pathway described here is implicated in more complex behaviors, or whether analogous descending pathways emerge from other regions of the dSC (perhaps supporting physiological components of other SC-mediated innate behaviors) remains to be seen. Like the cl-dSC, the rostromedial SC contains visually responsive neurons that project to the ipsilateral mRF, many of which are also activated by auditory and somatosensory stimuli (Isa et al., 2020; Westby et al., 1990). However, it is not yet clear whether descending efferents from the medial dSC contribute to respiratory or autonomic pathways: whereas early studies found equivalent pressor responses to electrical stimulation of the medial and lateral dSC (Keay et al., 1988), subsequent pharmacological studies found reactive sites were concentrated in the lateral dSC (Iigaya et al., 2012; Keay et al., 1990; Müller-Ribeiro et al., 2014).

In conclusion, the results of the current study demonstrate that the caudolateral dSC co-activates motor and physiological outputs that mimic those observed during alerting and orienting behaviors. These responses are largely reproduced by stimulation of dSC axons in the mRF, a critical relay nucleus for driving motor responses to SC-mediated orienting. In driving autonomic components of descending orienting pathways, this disynaptic pathway potentially primes physiological systems for future phases of arousal/flight or fight behavior independent of cortico-limbic and hypothalamic components of the classic defense pathway.

Figures

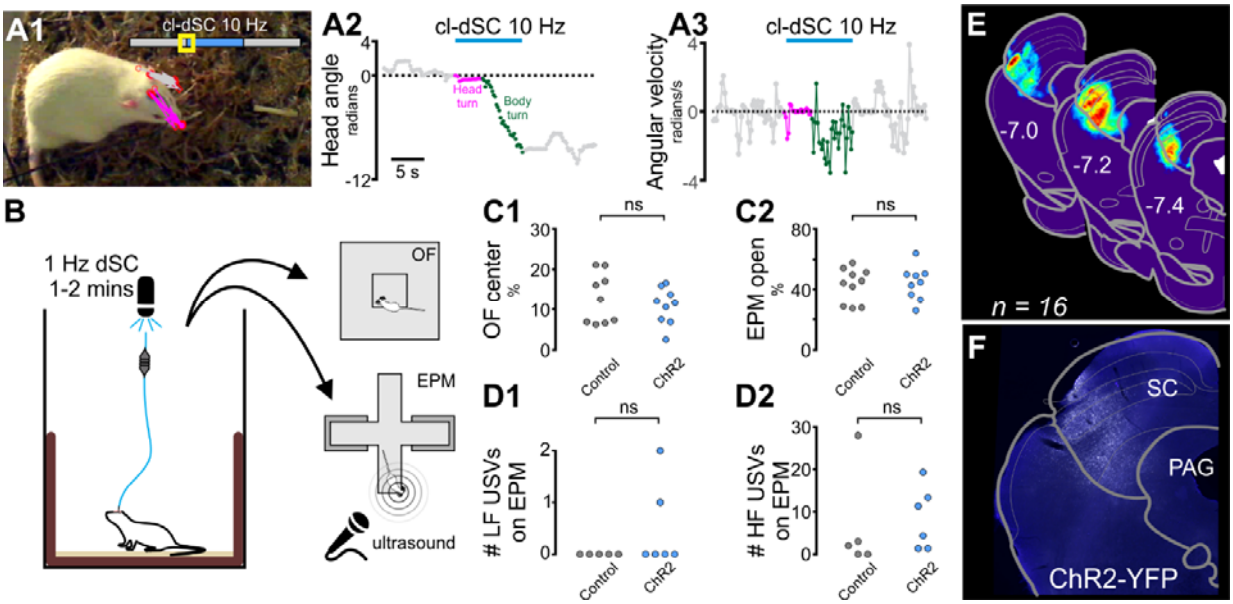

Figure 1 Caudolateral dSC stimulation evokes orienting responses but not anxiety-like behavior. A. Video-tracking shows typical response to moderate-intensity cl-dSC stimulation in ChR2-treated rat, characterized by immediate immobility and contraversive head-turning which transitions into full-body turning. A1 shows head position after 1 s of stimulation; head position in video frames denoted by the yellow box on the time scale is indicated by gray (baseline) and magenta (stimulation) arrows. A2-3 show head angle and angular velocity during the same experiment. B. The presence of anxiety-like behaviors were assayed immediately after optical cl-dSC stimulation using the open field (OF, C1) or elevated plus maze (EPM, C2) apparatus: no significant difference was detected between rats treated with ChR2 or control vectors. Similarly no effects on incidence of low- or high-frequency ultrasonic vocalizations (USVs) were detected while exploring the EPM (D1 & 2). E. Distribution of normalized ChR2-YFP fluorescence in 16 animals; representative example shown in panel F. ns = not significant. Gray circles here and throughout indicate animals injected with control vectors; blue circles indicate animals injected with AAV-Syn-ChR2-YFP.

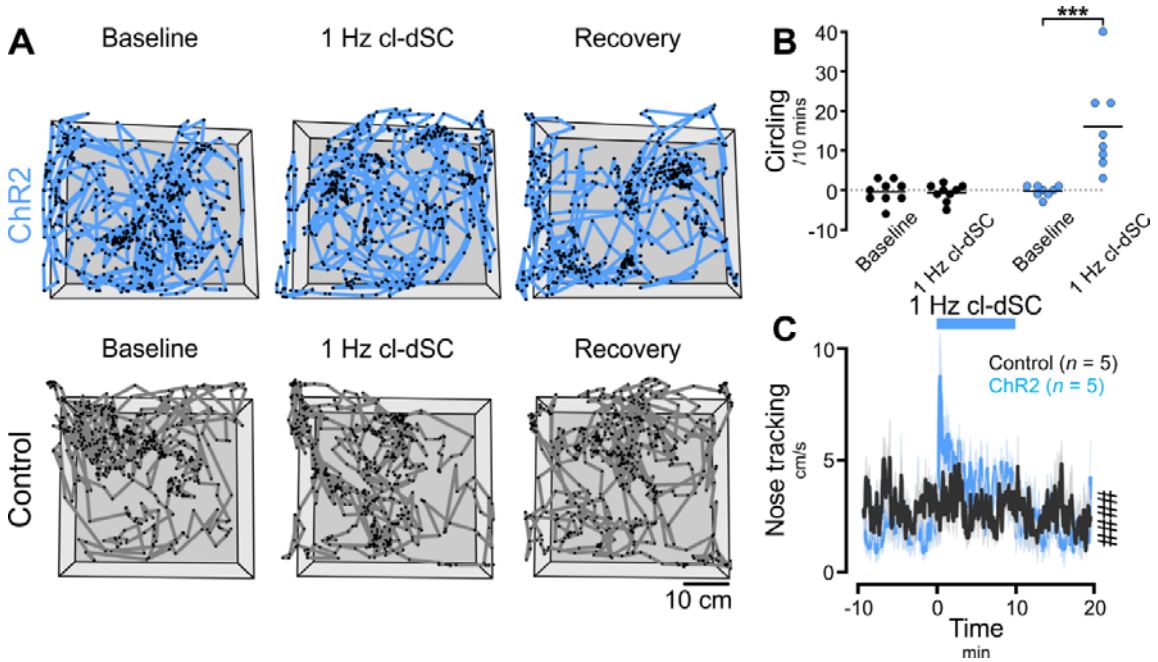

Figure 2 Behavioral responses to low frequency cl-dSC stimulation in rats injected with ChR2 and control vectors. A Examples of tracked nose position before, during and after 10 mins 1 Hz cl-dSC stimulation; in ChR2-treated animals cl-dSC stimulation was associated with contraversive orienting (B) and increased distance travelled (C), particularly during the first two minutes of stimulation. Gray boxes in A denote floor and walls of home cage; ***: P<0.001 paired t-test, ####: interaction P<0.0001, 2-way RM ANOVA. SEM here and elsewhere indicated by lighter shading.

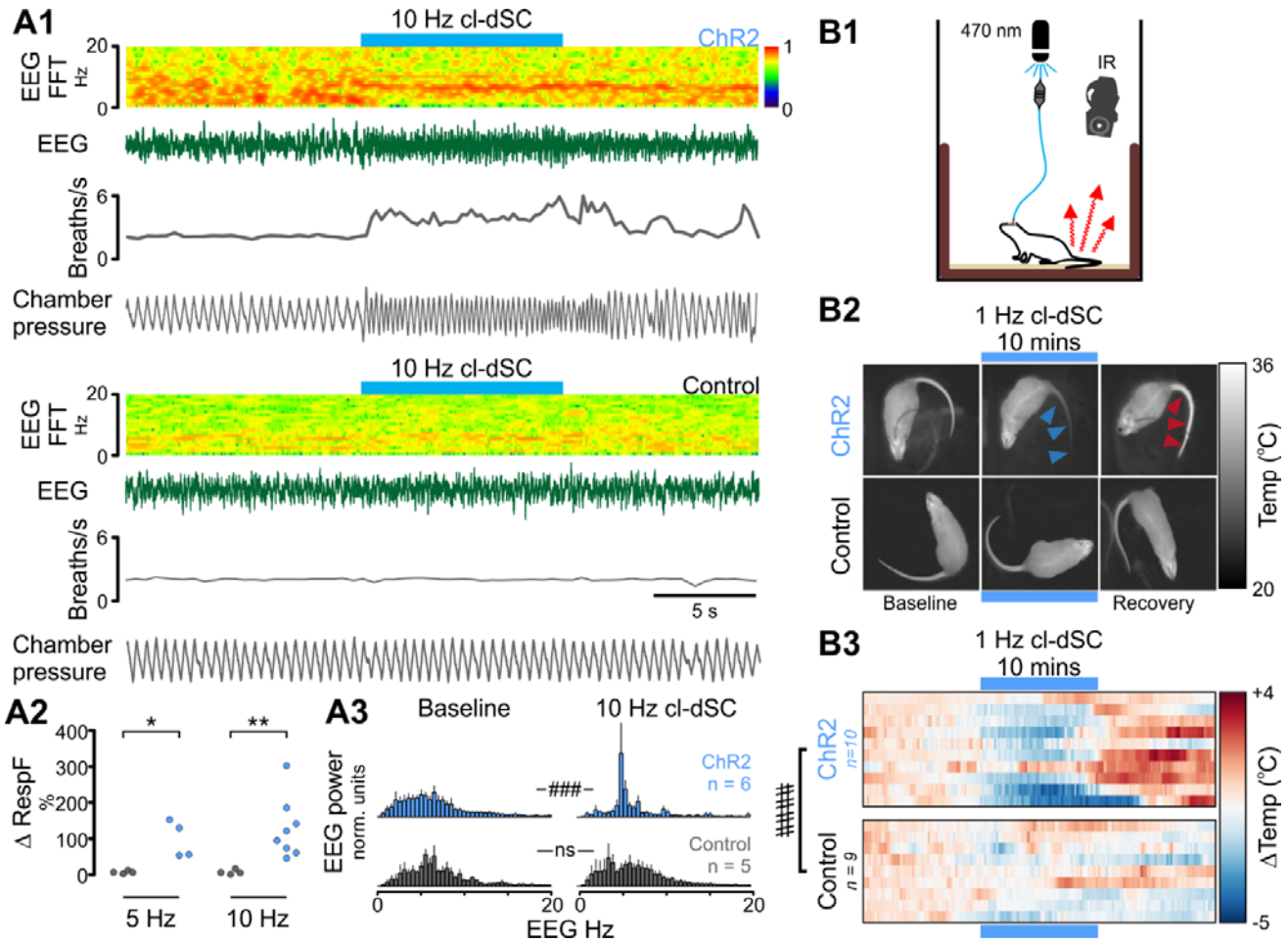

Figure 3 cl-dSC stimulation drives arousal, ventilation, and tail vasoconstriction in ChR2-treated but not in vector control rats. A1. Simultaneous recording of electroencephalogram (EEG) and respiratory rate from ChR2 (upper) and control vector treated (lower panels) animals showing tachypnoea and EEG desynchronization (0.5 - 4.5 Hz) with increased theta power (5-8 Hz). Pooled data shown in A2 (respiratory rate) and A3 (EEG frequency). B1. Tail temperature was measured by infra-red thermography before, during and after 10 minutes of 1 Hz cl-dSC stimulation. B2. Thermal imagery illustrates tail-cooling in ChR2 (blue arrowheads) experiment during stimulation, and tail temperature rebound (red arrowheads) during the recovery period. B3. Heat maps illustrate recordings from 10 ChR2 and 8 control vector treated rats: each row represents an individual experiment. *, **: Mann Whitney P<0.05, 0.01, ###, ####: 2-way RM ANOVA interaction P<0.001, <0.0001.

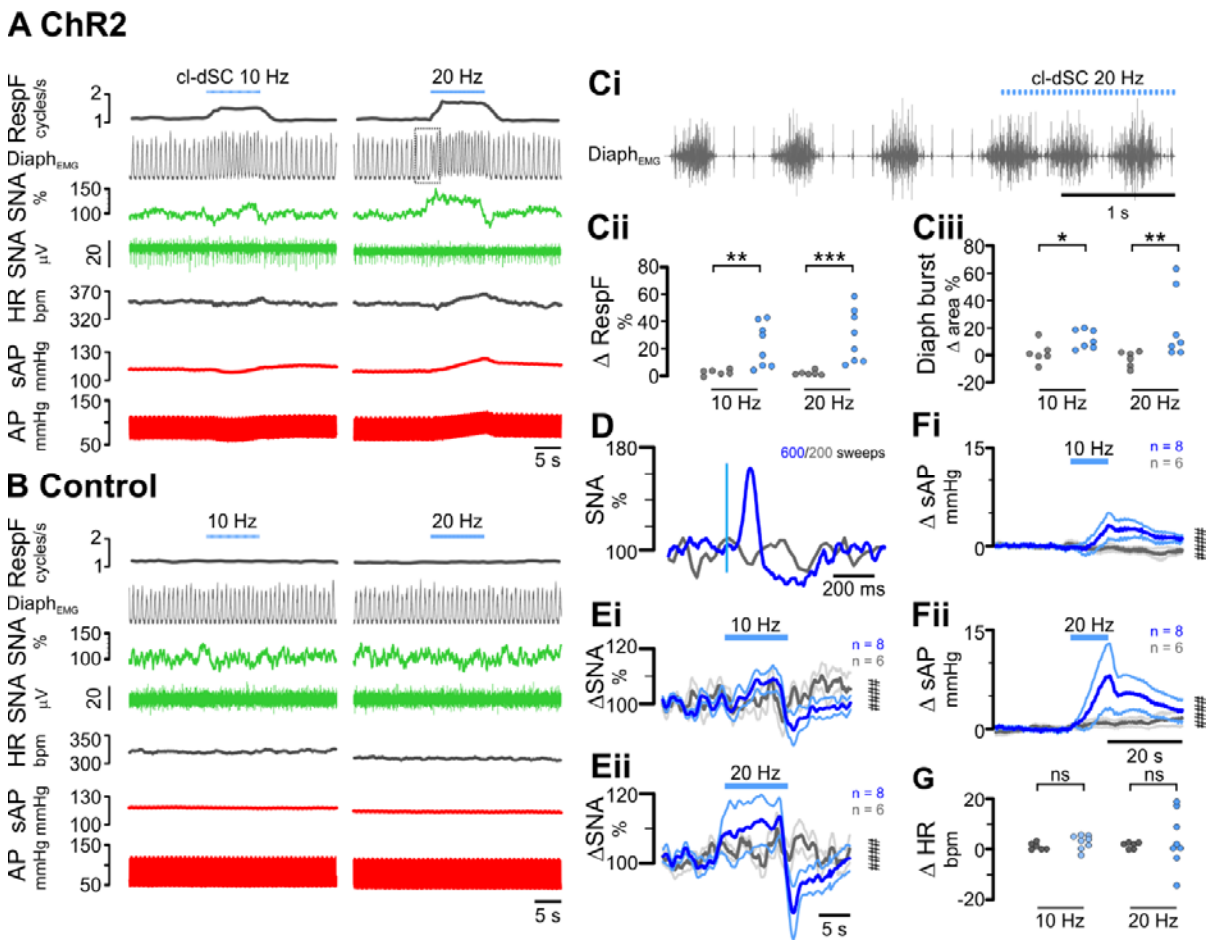

Figure 4 Respiratory and cardiovascular effects of cl-dSC stimulation under urethane anesthesia. Representative recordings from rats treated with ChR2 (A) and control (B) vectors. Boxed region in Panel A denotes expanded trace shown in Panel Ci. Respiratory effects (Panel C) manifested as an increase in diaphragmatic EMG burst frequency (Cii) and amplitude (Ciii). Single-pulse cl-dSC stimulation evoked short-latency monophasic bursts in SNA (D: vertical blue line denotes laser onset); repetitive cl-dSC stimulation evoked frequency-dependent recruitment of SNA (E) and systolic blood pressure (sAP, F), with variable effects on heart rate (HR: G). Bold traces in E & F indicate mean, light traces indicate SEM. *, **, *: Mann Whitney P<0.05, <0.01, <0.001; ####: 2-way RM ANOVA interaction P<0.0001.**

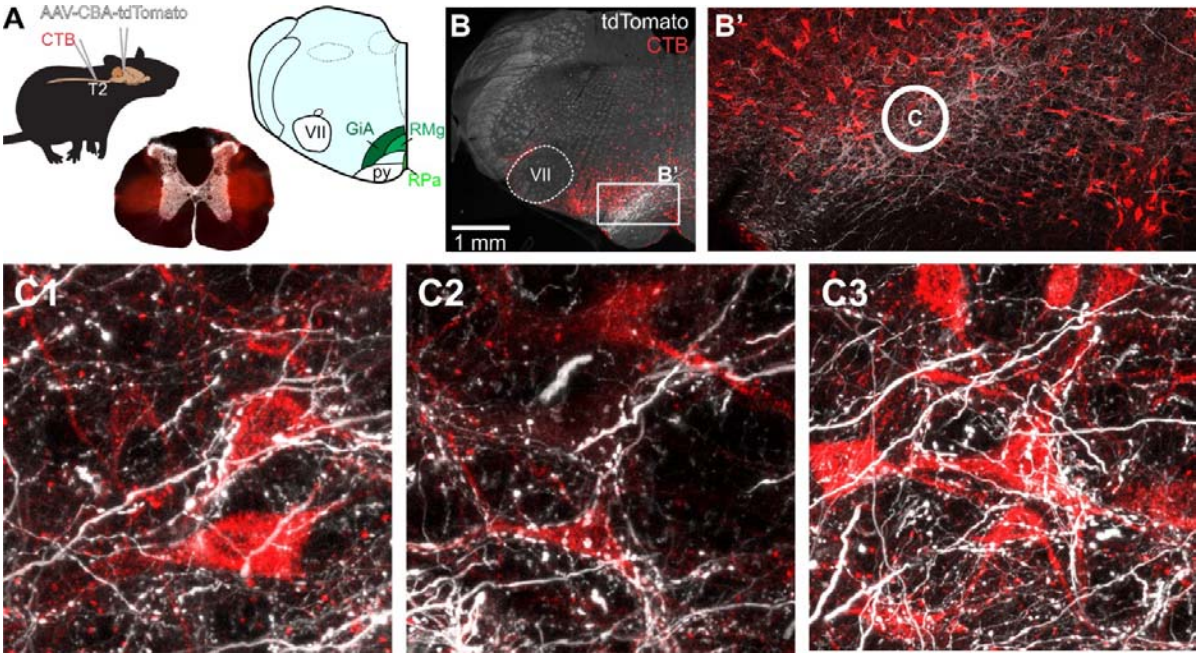

Figure 5 cl-dSC projections to spinally projecting neurons in the ventromedial medulla: A. Tracing strategy: AAV-CBA-tdTomato was used for anterograde labelling of cl-dSC neurons (white channel in B &C); microinjection of CTB at the thoracic intermediolateral cell column was used for retrograde labelling of bulbospinal neurons (red channel, brightfield photomicrograph in A shows CTB injection sites). cl-dSC injections resulted in extensive and predominantly ipsilateral terminal field labelling in the mRF (B), dorsal to the pyramidal tract (py), spanning the region from the midline raphe magnus (RMg) to the lateral gigantocellular reticular nucleus (GiA: B'). C. High-power confocal images of CTB-labelled GiA neurons from the circled region in B' in close apposition to cl-dSC terminals. VII: facial nucleus; RPa: raphe pallidus.

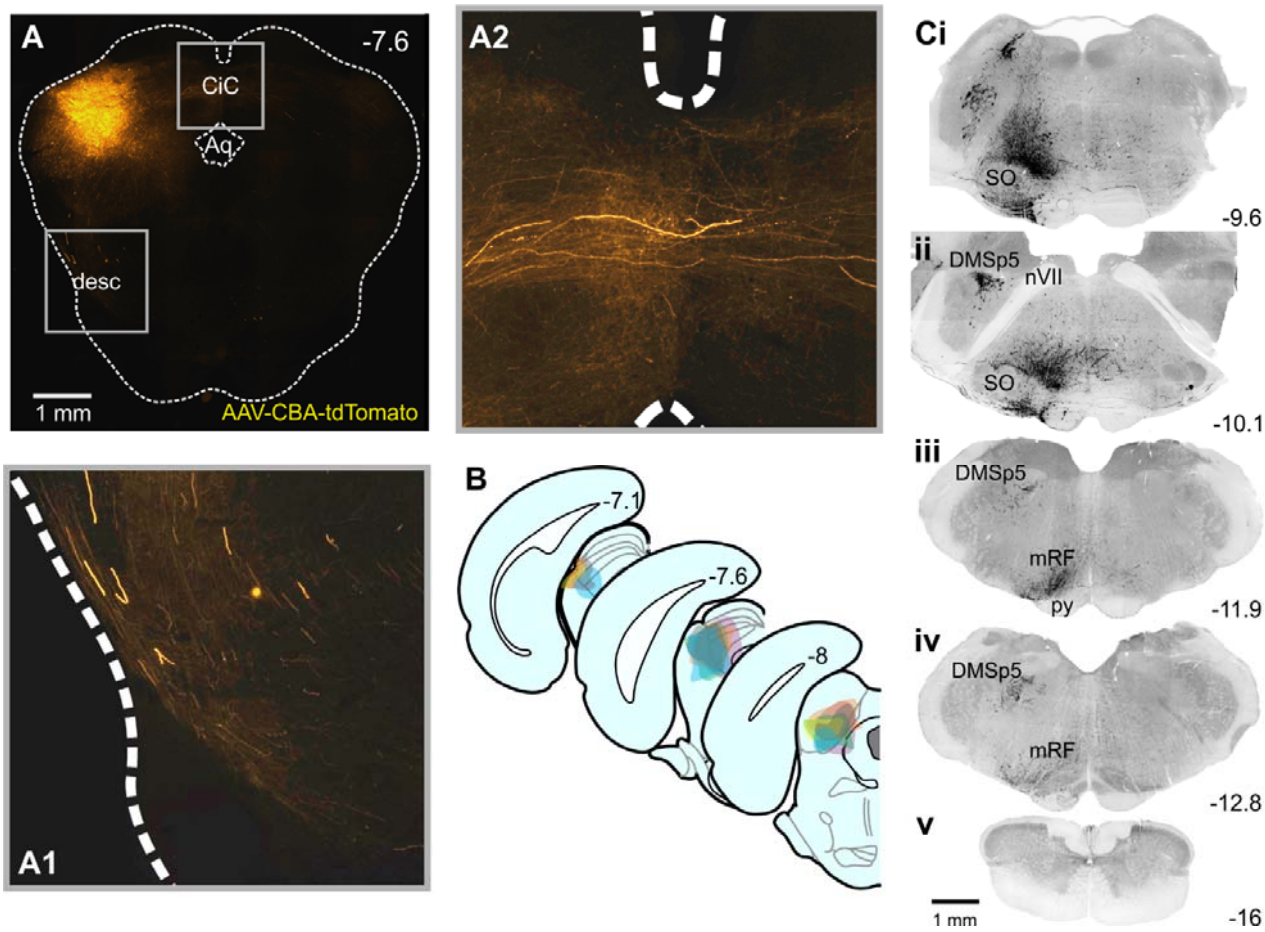

Figure 5 S1 Anterograde labelling from the cl-dSC: A. Example of AAV-CBA-tdTomato injection site in the cl-dSC. B. Composite diagram showing distribution of injection sites in 6 experiments. C. Shows histological sections from one experiment, illustrating the brainstem distribution of tdTomato labelling. Fibers emerging from the injection site followed either a descending trajectory via the lateral midbrain (desc, A1), or to the contralateral colliculi via the commissure of the inferior colliculus (CiC, A2). The descending bundle split into two tracts in the pons, a more substantial ventral bundle which emerged in the brainstem, surrounding the superior olive on all sides (SO, Ci), and a lesser and exclusively ipsilateral dorsal tract that innervated the dorsomedial spinal trigeminal nucleus (DMSp5, Cii) with large caliber fibers. The ventral branch occupied a column extending from the ventral surface to an apex at locus coeruleus (see Figure 5S2, panel C), was sparsely mirrored on the contralateral brainstem, and comprised both large and fine caliber fibers and putative terminals. Caudal to the facial nerve (nVII, Cii) the ventral branch was most densely concentrated in the medullary reticular formation (mRF, Ciii) dorsal to the pyramidal tract (py) at the level of the caudal pole of the facial nucleus. Labelled fibers were infrequently encountered in the caudal medulla (Civ) and virtually absent in spinal sections (Cv). Coordinates indicate rostrocaudal position with respect to Bregma.

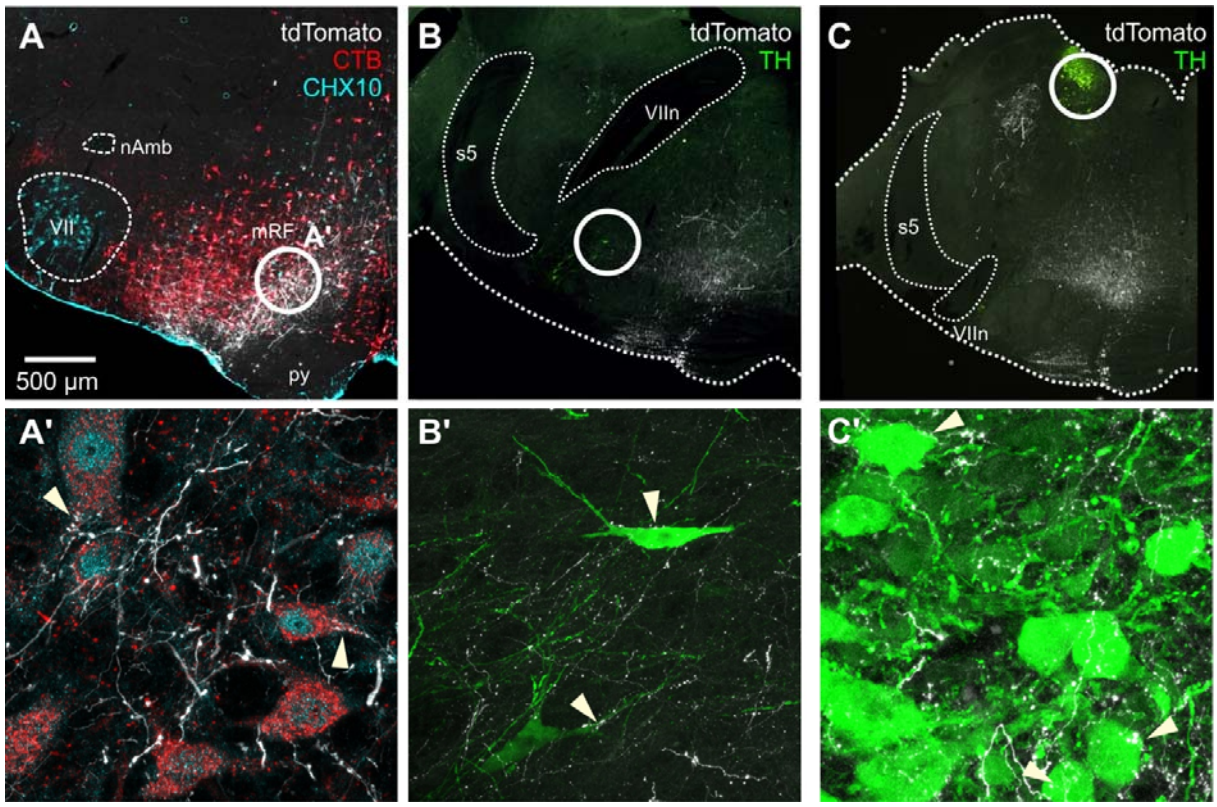

Figure 5S2: Phenotypes of putative targets of cl-dSC outputs, labelled by AAV-CBA-tdTomato: top row identifies region of interest (circled), lower panels highlight putative close appositions with CHX10 bulbospinal neurons in the mRF (identified by retrograde transport of CTB: A) and tyrosine hydroxylase (TH) immunoreactive neurons in the A5 (B), and A6 (C) cell groups.

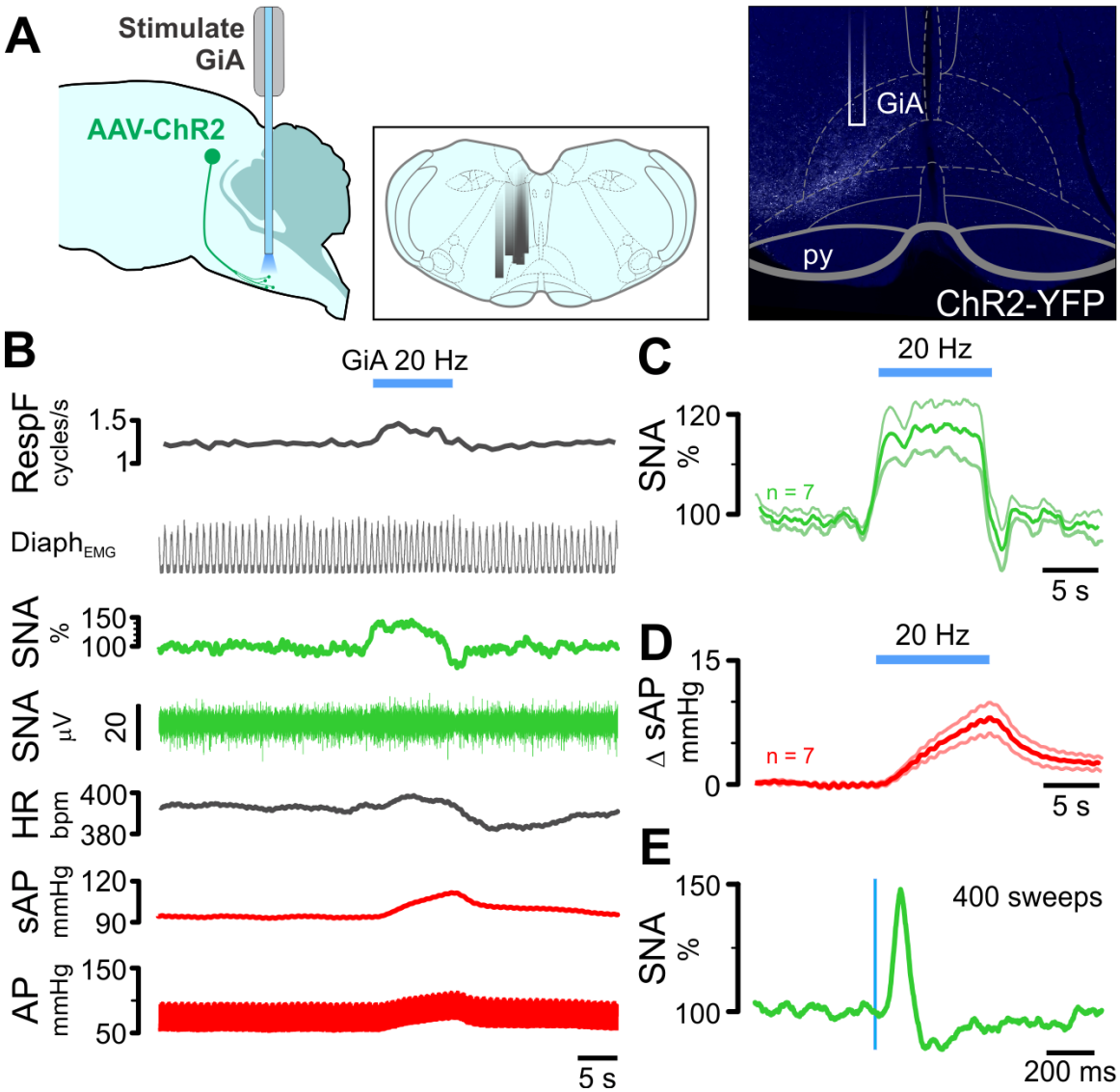

Figure 6 Respiratory and cardiovascular responses to optogenetic stimulation of cl-dSC-GiA terminals under urethane anesthesia. Panel A illustrates (L-R) experimental strategy, locations of fiber optic cannulae in different experiments, and example illustrating cannula position and terminal ChR2 labelling. B. Physiological recording of respiratory, sympathetic and cardiovascular responses to GiA stimulation; pooled sympathetic and pressor responses from 7 experiments are shown in C & D. E. Shows stimulus-triggered average of sympathetic response to 0.5 Hz stimulation from the experiment shown in B.

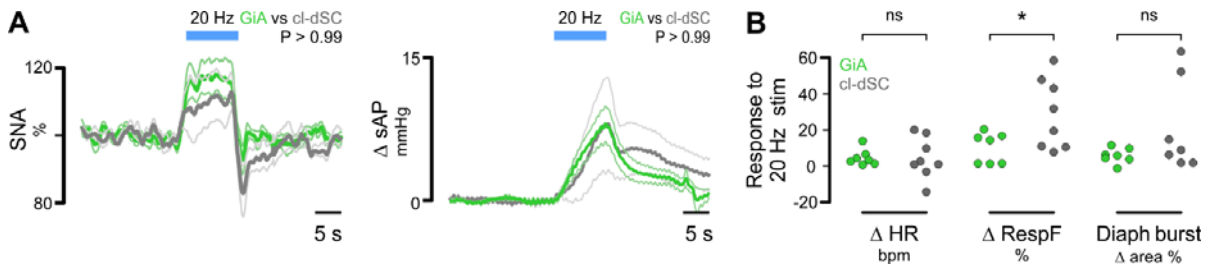

Figure 6 S1 Direct comparison of responses evoked by optogenetic stimulation of cl-dSC neurons (dark gray) and their GiA terminals (green). Outputs examined were sympathetic nerve activity & systolic blood pressure (A), and heart rate, respiratory frequency and respiratory burst area (B). Significantly different responses were only detected in respiratory frequency (*: P<0.05, unpaired t-test).

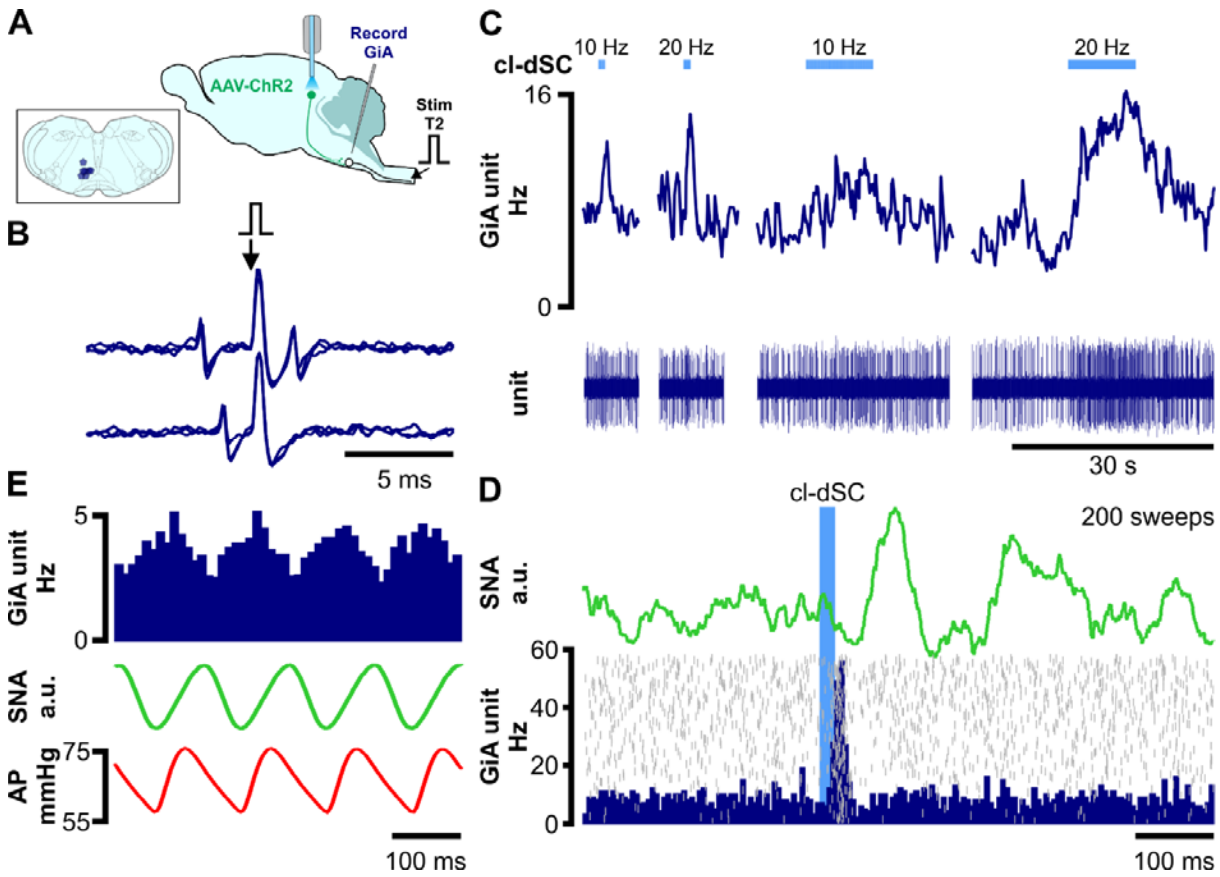

Figure 7 Optogenetic cl-dSC stimulation activates spinally projecting cardiovascular and non-cardiovascular GiA neurons. A. Extracellular recordings were made from bulbospinal GiA neurons under urethane anesthesia after transduction of cl-dSC neurons with ChR2 and fiber optic implantation; inset shows recording sites of 7 neurons. B. All spinally projecting neurons exhibited constant-latency antidromic spikes in response to electrical stimulation of the T2 spinal cord (top trace) which collided with spontaneous orthodromic spikes (lower trace). C. cl-dSC stimulation evoked frequency-dependent increases in baseline activity: trace shows typical responses to short (1s) and long (10 s) trains of stimulation at 10 and 20 Hz (same neuron as B). D. Low-frequency cl-dSC stimulation evoked short-latency response in the same neuron (lower panel) that preceded simultaneously recorded sympathoexcitation (green trace). E. Putative sympathetic premotor neurons were identified by covariation in neuronal activity (top trace) with SNA (green) and pulsatile arterial pressure (lower trace).

Acknowledgments

This work was funded by the National Health & Medical Research Council (APP2001128, APP1127817), the Hillcrest Foundation (IPAP2019_0933, IPAP2018_0437) and by Macquarie University. EL, BD & CS were Macquarie University postgraduate scholars. The authors are grateful to Pascal Carrive, for providing access to his precious thermal camera with patience and grace, and to Nick Everett for the use of his ultrasonic microphone.

Author Contributions

EL: stereotaxic injections & optrode implantation, behavioral, plethysmography & electrophysiological experiments, data analysis & manuscript draft. BD: anterograde tracing, imaging & analysis, drafting of results. EM: behavioral experiments, tail thermography & analysis, drafting of results, histological reconstruction & imaging. AT: stereotaxic injections, optrode implantations & electrophysiological recordings. CS: histology, imaging and validation. PB: EEG & plethysmography experiments. AA: AAV-CBA-tdTomato design & construction, drafting of the manuscript. RD: Conceptualization, experimental design, interpretation, drafting of the manuscript and funding. CH: conceptualization & interpretation. JC: supervision and interpretation of behavioral & USV recordings, funding. AKG: conceptualization, supervision & interpretation of tracing experiments, drafting of the manuscript & funding. SM: conceptualization, supervision of electrophysiology experiments, data analysis, drafting of the manuscript & funding. All authors edited the manuscript.

Declaration of Interests

None to declare

References

Abbott, S.B., Stornetta, R.L., Socolovsky, C.S., West, G.H., and Guyenet, P.G. (2009). Photostimulation of channelrhodopsin-2 expressing ventrolateral medullary neurons increases sympathetic nerve activity and blood pressure in rats. J Physiol 587, 5613-5631.

Abe, C., Inoue, T., Inglis, M.A., Viar, K.E., Huang, L., Ye, H., Rosin, D.L., Stornetta, R.L., Okusa, M.D., and Guyenet, P.G. (2017). C1 neurons mediate a stress-induced anti-inflammatory reflex in mice. Nat Neurosci 20, 700-707.

Basso, M.A., and May, P.J. (2017). Circuits for Action and Cognition: A View from the Superior Colliculus. Annu Rev Vis Sci 3, 197-226.

Baudrie, V., Tulen, J.H., Blanc, J., and Elghozi, J.L. (1997). Autonomic components of the cardiovascular responses to an acoustic startle stimulus in rats. J Auton Pharmacol 17, 303-309.

Boehnke, S.E., and Munoz, D.P. (2008). On the importance of the transient visual response in the superior colliculus. Curr Opin Neurobiol 18, 544-551.

Bouvier, J., Caggiano, V., Leiras, R., Caldeira, V., Bellardita, C., Balueva, K., Fuchs, A., and Kiehn, O. (2015). Descending Command Neurons in the Brainstem that Halt Locomotion. Cell 163, 1191-1203.

Brudzynski, S.M. (2007). Ultrasonic calls of rats as indicator variables of negative or positive states: acetylcholine-dopamine interaction and acoustic coding. Behav Brain Res 182, 261-273.

Brudzynski, S.M. (2013). Ethotransmission: communication of emotional states through ultrasonic vocalization in rats. Current Opinion in Neurobiology 23, 310-317.

Butler, A.B., and Hodos, W. (2005). Comparative vertebrate neuroanatomy: evolution and adaptation, Second Edition edn (John Wiley & Sons).

Buzsáki, G. (2006). Rhythms of the Brain (Oxford University Press, Inc.).

Cano, G., Sved, A.F., Rinaman, L., Rabin, B.S., and Card, J.P. (2001). Characterization of the central nervous system innervation of the rat spleen using viral transneuronal tracing. J Comp Neurol 439, 1-18.

Caraffa-Braga, E., Granata, L., and Pinotti, O. (1973). Changes in blood-flow distribution during acute emotional stress in dogs. Pflugers Arch 339, 203-216.

Card, J.P., Kobiler, O., McCambridge, J., Ebdlahad, S., Shan, Z., Raizada, M.K., Sved, A.F., and Enquist, L.W. (2011). Microdissection of neural networks by conditional reporter expression from a Brainbow herpesvirus. Proceedings of the National Academy of Sciences of the United States of America 108, 3377-3382.

Casto, R., and Printz, M.P. (1990). Exaggerated response to alerting stimuli in spontaneously hypertensive rats. Hypertension 16, 290-300.

Chamberlin, N., and Saper, C. (1994). Topographic organization of respiratory responses to glutamate microstimulation of the parabrachial nucleus in the rat. The Journal of Neuroscience 14, 6500-6510.

Chen, Q.H., and Toney, G.M. (2010). In vivo discharge properties of hypothalamic paraventricular nucleus neurons with axonal projections to the rostral ventrolateral medulla. J Neurophysiol 103, 4-15.

Comoli, E., Das Neves Favaro, P., Vautrelle, N., Leriche, M., Overton, P., and Redgrave, P. (2012). Segregated Anatomical Input to Sub-Regions of the Rodent Superior Colliculus Associated with Approach and Defense. Frontiers in Neuroanatomy 6.

Crone, S.A., Quinlan, K.A., Zagoraiou, L., Droho, S., Restrepo, C.E., Lundfald, L., Endo, T., Setlak, J., Jessell, T.M., Kiehn, O., and Sharma, K. (2008). Genetic ablation of V2a ipsilateral interneurons disrupts left-right locomotor coordination in mammalian spinal cord. Neuron 60, 70-83.

Crone, S.A., Viemari, J.C., Droho, S., Mrejeru, A., Ramirez, J.M., and Sharma, K. (2012). Irregular Breathing in Mice following Genetic Ablation of V2a Neurons. J Neurosci 32, 7895-7906.

Crone, S.A., Zhong, G., Harris-Warrick, R., and Sharma, K. (2009). In mice lacking V2a interneurons, gait depends on speed of locomotion. J Neurosci 29, 7098-7109.

Dampney, R.A. (1994). Functional organization of central pathways regulating the cardiovascular system. Physiological Reviews 74, 323-364.

Dampney, R.A., Horiuchi, J., and McDowall, L.M. (2008). Hypothalamic mechanisms coordinating cardiorespiratory function during exercise and defensive behaviour. Auton Neurosci 142, 3-10.

de Menezes, R.C., Ootsuka, Y., and Blessing, W.W. (2009). Sympathetic cutaneous vasomotor alerting responses (SCVARs) are associated with hippocampal theta rhythm in non-moving conscious rats. Brain Res 1298, 123-130.

Dean, P., Redgrave, P., and Westby, G.W.M. (1989). Event or emergency? Two response systems in the mammalian superior colliculus. Trends in Neurosciences 12, 137-147.

Dempsey, B., Le, S., Turner, A., Bokiniec, P., Ramadas, R., Bjaalie, J.G., Menuet, C., Neve, R., Allen, A.M., Goodchild, A.K., and McMullan, S. (2017). Mapping and Analysis of the Connectome of Sympathetic Premotor Neurons in the Rostral Ventrolateral Medulla of the Rat Using a Volumetric Brain Atlas. Front Neural Circuits 11, 9.

Depuy, S.D., Kanbar, R., Coates, M.B., Stornetta, R.L., and Guyenet, P.G. (2011). Control of breathing by raphe obscurus serotonergic neurons in mice. J Neurosci 31, 1981-1990.

Dougherty, K.J., and Kiehn, O. (2010). Functional organization of V2a-related locomotor circuits in the rodent spinal cord. Ann N Y Acad Sci 1198, 85-93.

Furigo, I.C., de Oliveira, W.F., de Oliveira, A.R., Comoli, E., Baldo, M.V., Mota-Ortiz, S.R., and Canteras, N.S. (2010). The role of the superior colliculus in predatory hunting. Neuroscience 165, 1-15.

Furlong, T.M., McDowall, L.M., Horiuchi, J., Polson, J.W., and Dampney, R.A. (2014). The effect of air puff stress on c-Fos expression in rat hypothalamus and brainstem: central circuitry mediating sympathoexcitation and baroreflex resetting. Eur J Neurosci 39, 1429-1438.

Guyenet, P.G. (2006). The sympathetic control of blood pressure. Nat Rev Neurosci 7, 335-346.

Guyenet, P.G., Stornetta, R.L., Bochorishvili, G., Depuy, S.D., Burke, P.G., and Abbott, S.B. (2013). C1 neurons: the body's EMTs. Am J Physiol Regul Integr Comp Physiol 305, R187-204.

Hayward, L.F., Swartz, C.L., and Davenport, P.W. (2003). Respiratory response to activation or disinhibition of the dorsal periaqueductal gray in rats. J Appl Physiol (1985) 94, 913-922.

Iigaya, K., Müller-Ribeiro, F.C., Horiuchi, J., McDowall, L.M., Nalivaiko, E., Fontes, M.A., and Dampney, R.A. (2012). Synchronized activation of sympathetic vasomotor, cardiac, and respiratory outputs by neurons in the midbrain colliculi. Am J Physiol Regul Integr Comp Physiol 303, R599-610.

Isa, K., Sooksawate, T., Kobayashi, K., Kobayashi, K., Redgrave, P., and Isa, T. (2020). Dissecting the tectal output channels for orienting and defense responses. eNeuro, ENEURO.0271-0220.2020.

Isa, T., and Sasaki, S. (2002). Brainstem control of head movements during orienting; organization of the premotor circuits. Progress in Neurobiology 66, 205-241.

Kabir, M.M., Beig, M.I., Baumert, M., Trombini, M., Mastorci, F., Sgoifo, A., Walker, F.R., Day, T.A., and Nalivaiko, E. (2010). Respiratory pattern in awake rats: effects of motor activity and of alerting stimuli. Physiol Behav 101, 22-31.

Kataoka, N., Shima, Y., Nakajima, K., and Nakamura, K. (2020). A central master driver of psychosocial stress responses in the rat. Science 367, 1105-1112.

Keay, K.A., Dean, P., and Redgrave, P. (1990). N-methyl D-aspartate (NMDA) evoked changes in blood pressure and heart rate from the rat superior colliculus. Exp Brain Res 80, 148-156.

Keay, K.A., Redgrave, P., and Dean, P. (1988). Cardiovascular and respiratory changes elicited by stimulation of rat superior colliculus. Brain Res Bull 20, 13-26.

Kerman, I.A. (2008). Organization of brain somatomotor-sympathetic circuits. Exp Brain Res 187, 1-16.

Kim, L.H., Sharma, S., Sharples, S.A., Mayr, K.A., Kwok, C.H.T., and Whelan, P.J. (2017). Integration of Descending Command Systems for the Generation of Context-Specific Locomotor Behaviors. Frontiers in neuroscience 11.

Krauzlis, R.J., Bogadhi, A.R., Herman, J.P., and Bollimunta, A. (2018). Selective attention without a neocortex. Cortex; a journal devoted to the study of the nervous system and behavior 102, 161-175.

May, P.J. (2006). The mammalian superior colliculus: laminar structure and connections. Prog Brain Res 151, 321-378.

McMullan, S., Goodchild, A.K., and Pilowsky, P.M. (2007). Circulating angiotensin II attenuates the sympathetic baroreflex by reducing the barosensitivity of medullary cardiovascular neurones in the rat. J Physiol 582, 711-722.

Menuet, C., Sevigny, C.P., Connelly, A.A., Bassi, J.K., Jancovski, N., Williams, D.A., Anderson, C.R., Llewellyn-Smith, I.J., Fong, A.Y., and Allen, A.M. (2014). Catecholaminergic C3 neurons are sympathoexcitatory and involved in glucose homeostasis. J Neurosci 34, 15110-15122.

Meredith, M.A., and Stein, B.E. (1986). Visual, auditory, and somatosensory convergence on cells in superior colliculus results in multisensory integration. J Neurophysiol 56, 640-662.

Morris, K.F., Arata, A., Shannon, R., and Lindsey, B.G. (1996). Long-term facilitation of phrenic nerve activity in cats: responses and short time scale correlations of medullary neurones. J Physiol 490 (Pt 2), 463-480.

Morrison, S.F. (1999). RVLM and raphe differentially regulate sympathetic outflows to splanchnic and brown adipose tissue. American Journal of Physiology-Regulatory Integrative and Comparative Physiology 276, R962-R973.

Morrison, S.F., Milner, T.A., and Reis, D.J. (1988). Reticulospinal vasomotor neurons of the rat rostral ventrolateral medulla: relationship to sympathetic nerve activity and the C1 adrenergic cell group. J Neurosci 8, 1286-1301.

Müller-Ribeiro, F.C., Dampney, R.A., McMullan, S., Fontes, M.A., and Goodchild, A.K. (2014). Disinhibition of the midbrain colliculi unmasks coordinated autonomic, respiratory, and somatomotor responses to auditory and visual stimuli. Am J Physiol Regul Integr Comp Physiol 307, R1025-1035.

Müller-Ribeiro, F.C., Goodchild, A.K., McMullan, S., Fontes, M.A., and Dampney, R.A. (2016). Coordinated autonomic and respiratory responses evoked by alerting stimuli: Role of the midbrain colliculi. Respir Physiol Neurobiol 226, 87-93.

Nalivaiko, E., Bondarenko, E., Lidstrom, A., and Barry, R. (2012). Respiratory Component of the Orienting Reflex: A Novel Sensitive Index of Sensory-Induced Arousal in Rats. Frontiers in physiology 2.

Ootsuka, Y., Mohammed, M., and Blessing, W.W. (2017). Lateral habenula regulation of emotional hyperthermia: mediation via the medullary raphe. Scientific reports 7, 4102.

Perreault, M.-C., and Giorgi, A. (2019). Diversity of reticulospinal systems in mammals. Current Opinion in Physiology 8, 161-169.

Porreca, F., Ossipov, M.H., and Gebhart, G.F. (2002). Chronic pain and medullary descending facilitation. Trends Neurosci 25, 319-325.

Rathner, J.A., and McAllen, R.M. (1999). Differential control of sympathetic drive to the rat tail artery and kidney by medullary premotor cell groups. Brain Res 834, 196-199.

Redgrave, P., Mitchell, I.J., and Dean, P. (1987). Descending projections from the superior colliculus in rat: a study using orthograde transport of wheatgerm-agglutinin conjugated horseradish peroxidase. Exp Brain Res 68, 147-167.

Rettig, R., Geyer, M.A., and Printz, M.P. (1986). Cardiovascular concomitants of tactile and acoustic startle responses in spontaneously hypertensive and normotensive rats. Physiol Behav 36, 1123-1128.

Sahibzada, N., Dean, P., and Redgrave, P. (1986). Movements resembling orientation or avoidance elicited by electrical stimulation of the superior colliculus in rats. J Neurosci 6, 723-733.

Saidel, W.M. (2009). Evolution of the Optic Tectum in Anamniotes. In Encyclopedia of Neuroscience, M.D. Binder, N. Hirokawa, and U. Windhorst, eds. (Berlin, Heidelberg: Springer Berlin Heidelberg), pp. 1380-1387.

Shang, C., Liu, A., Li, D., Xie, Z., Chen, Z., Huang, M., Li, Y., Wang, Y., Shen, W.L., and Cao, P. (2019). A subcortical excitatory circuit for sensory-triggered predatory hunting in mice. Nat Neurosci 22, 909-920.

Silva, B.A., Gross, C.T., and Graff, J. (2016). The neural circuits of innate fear: detection, integration, action, and memorization. Learn Mem 23, 544-555.

Soper, C., Wicker, E., Kulick, C.V., N'Gouemo, P., and Forcelli, P.A. (2016). Optogenetic activation of superior colliculus neurons suppresses seizures originating in diverse brain networks. Neurobiology of disease 87, 102-115.

Sparks, D.L., Lee, C., and Rohrer, W.H. (1990). Population coding of the direction, amplitude, and velocity of saccadic eye movements by neurons in the superior colliculus. Cold Spring Harbor symposia on quantitative biology 55, 805-811.

Standish, A., Enquist, L.W., Escardo, J.A., and Schwaber, J.S. (1995). Central neuronal circuit innervating the rat heart defined by transneuronal transport of pseudorabies virus. J Neurosci 15, 1998-2012.

Stein, B.E., and Meredith, M.A. (1993). The Merging of the Senses (MIT Press).

Stornetta, R.L. (2009). Neurochemistry of bulbospinal presympathetic neurons of the medulla oblongata. J Chem Neuroanat 38, 222-230.

Stornetta, R.L., Inglis, M.A., Viar, K.E., and Guyenet, P.G. (2015). Afferent and efferent connections of C1 cells with spinal cord or hypothalamic projections in mice. Brain structure & function.

Strack, A.M., Sawyer, W.B., Hughes, J.H., Platt, K.B., and Loewy, A.D. (1989). A general pattern of CNS innervation of the sympathetic outflow demonstrated by transneuronal pseudorabies viral infections. Brain Research 491, 156-162.

Turner, A., Kumar, N., Farnham, M., Lung, M., Pilowsky, P., and McMullan, S. (2013). Rostroventrolateral medulla neurons with commissural projections provide input to sympathetic premotor neurons: anatomical and functional evidence. Eur J Neurosci 38, 2504-2515.

Usseglio, G., Gatier, E., Heuze, A., Herent, C., and Bouvier, J. (2020). Control of Orienting Movements and Locomotion by Projection-Defined Subsets of Brainstem V2a Neurons. Current biology : CB 30, 4665-4681 e4666.

Varner, K.J., Rutherford, D.S., Vasquez, E.C., and Brody, M.J. (1992). Identification of cardiovascular neurons in the rostral ventromedial medulla in anesthetized rats. Hypertension 19, II193-197.

Verner, T.A., Goodchild, A.K., and Pilowsky, P.M. (2004). A mapping study of cardiorespiratory responses to chemical stimulation of the midline medulla oblongata in ventilated and freely breathing rats. Am J Physiol Regul Integr Comp Physiol 287, R411-421.

Vianna, D.M., Allen, C., and Carrive, P. (2008). Cardiovascular and behavioral responses to conditioned fear after medullary raphe neuronal blockade. Neuroscience 153, 1344-1353.

Vianna, D.M., and Carrive, P. (2005). Changes in cutaneous and body temperature during and after conditioned fear to context in the rat. Eur J Neurosci 21, 2505-2512.

Wei, P., Liu, N., Zhang, Z., Liu, X., Tang, Y., He, X., Wu, B., Zhou, Z., Liu, Y., Li, J., *et al.* (2015). Processing of visually evoked innate fear by a non-canonical thalamic pathway. Nat Commun 6, 6756.

Westby, G.W., Keay, K.A., Redgrave, P., Dean, P., and Bannister, M. (1990). Output pathways from the rat superior colliculus mediating approach and avoidance have different sensory properties. Exp Brain Res 81, 626-638.

Yilmaz, M., and Meister, M. (2013). Rapid innate defensive responses of mice to looming visual stimuli. Current biology : CB 23, 2011-2015.

Yu, Y.H., and Blessing, W.W. (1997). Cutaneous vasoconstriction in conscious rabbits during alerting responses detected by hippocampal theta-rhythm. American Journal of Physiology-Regulatory, Integrative and Comparative Physiology 272, R208-R216.

Zhao, Z., Wang, L., Gao, W., Hu, F., Zhang, J., Ren, Y., Lin, R., Feng, Q., Cheng, M., Ju, D., *et al.* (2017). A Central Catecholaminergic Circuit Controls Blood Glucose Levels during Stress. Neuron 95, 138-152 e135.

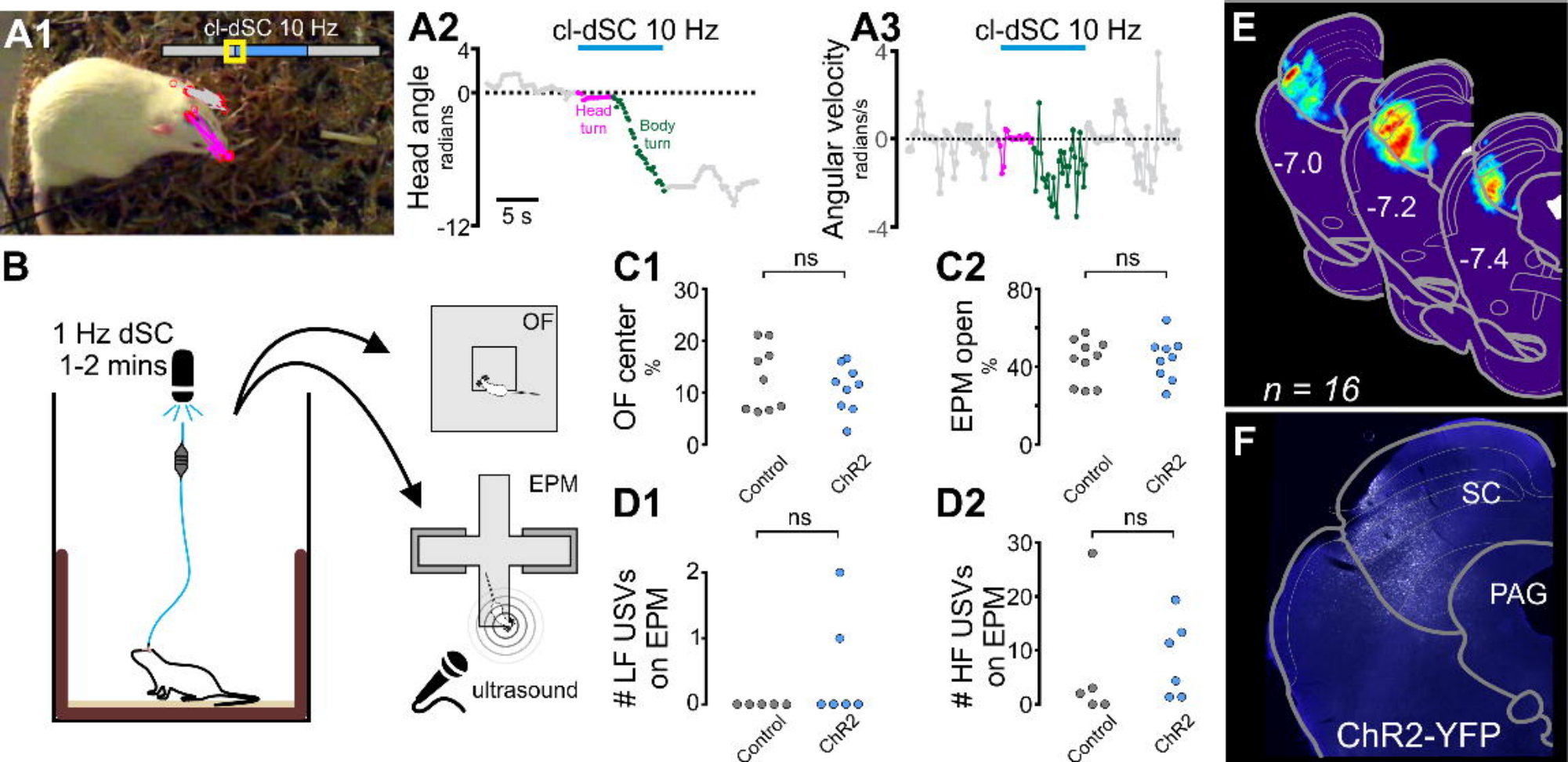
A1
cl-dSC 10 Hz
A2
cl-dSC 10 Hz
Head angle
radians
4
0
-12
Head turn
Body turn
5 s
A3
cl-dSC 10 Hz
Angular velocity
radians/s
4
0
-4
B
1 Hz dSC
1-2 mins
OF
EPM
ultrasound
C1
ns
OF center
%
30
20
10
0
Control
ChR2
C2
ns
EPM open
%
80
40
0
Control
ChR2
D1
ns
LF USVs on EPM
2
1
0
Control
ChR2
D2
ns
HF USVs on EPM
30
20
10
0
Control
ChR2
E
-7.0
-7.2
-7.4
n = 16
F
SC
PAG
ChR2-YFP

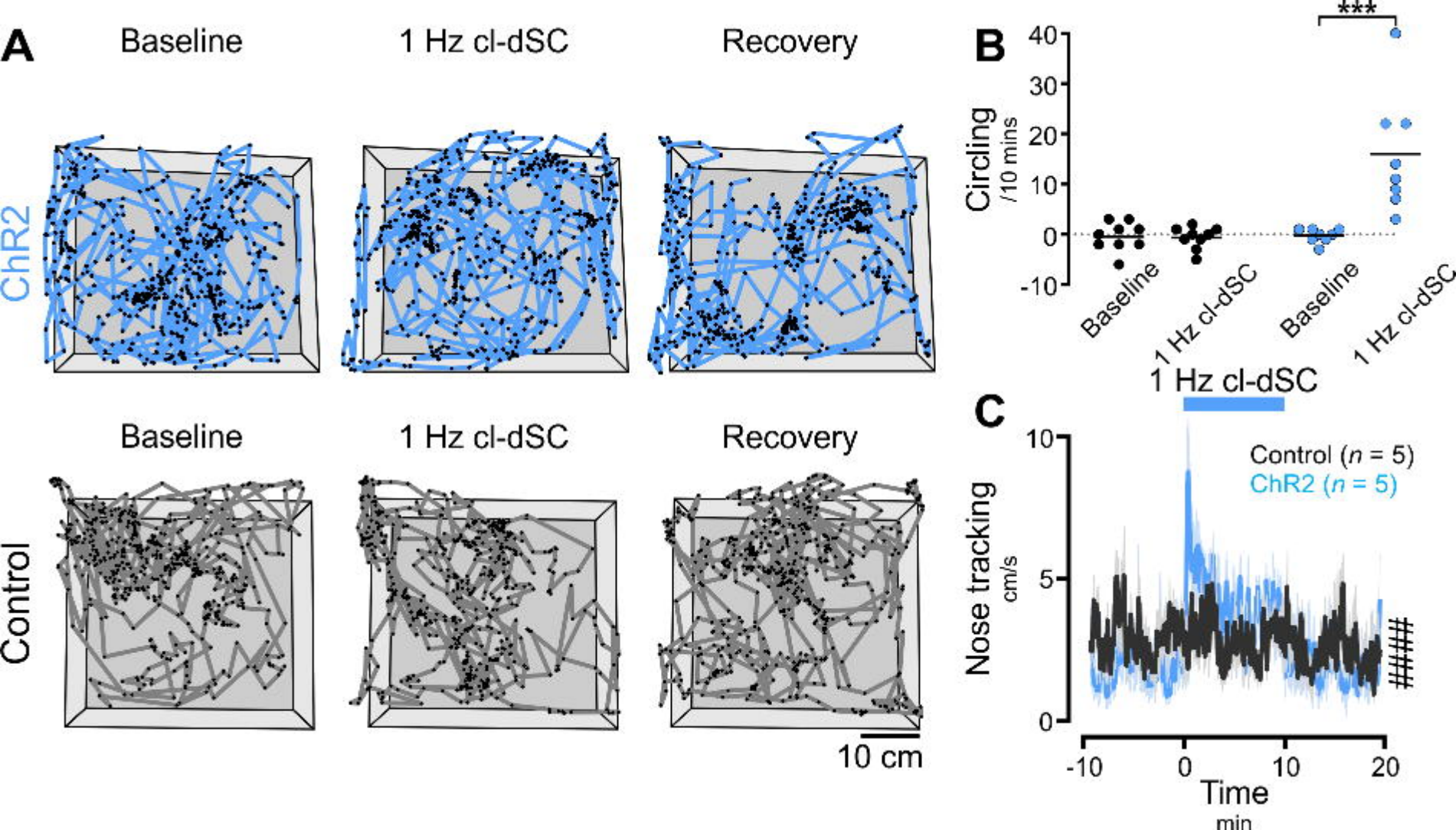
A
Baseline
1 Hz cl-dSC
Recovery
ChR2
Control
10 cm
B
Circling
/10 mins
40
30
20
10
0
-10
***
Baseline
1 Hz cl-dSC
Baseline
1 Hz cl-dSC
1 Hz cl-dSC
C
Control (n = 5)
ChR2 (n = 5)
Nose tracking
cm/s
10
5
0
-10
0
10
20
Time
min

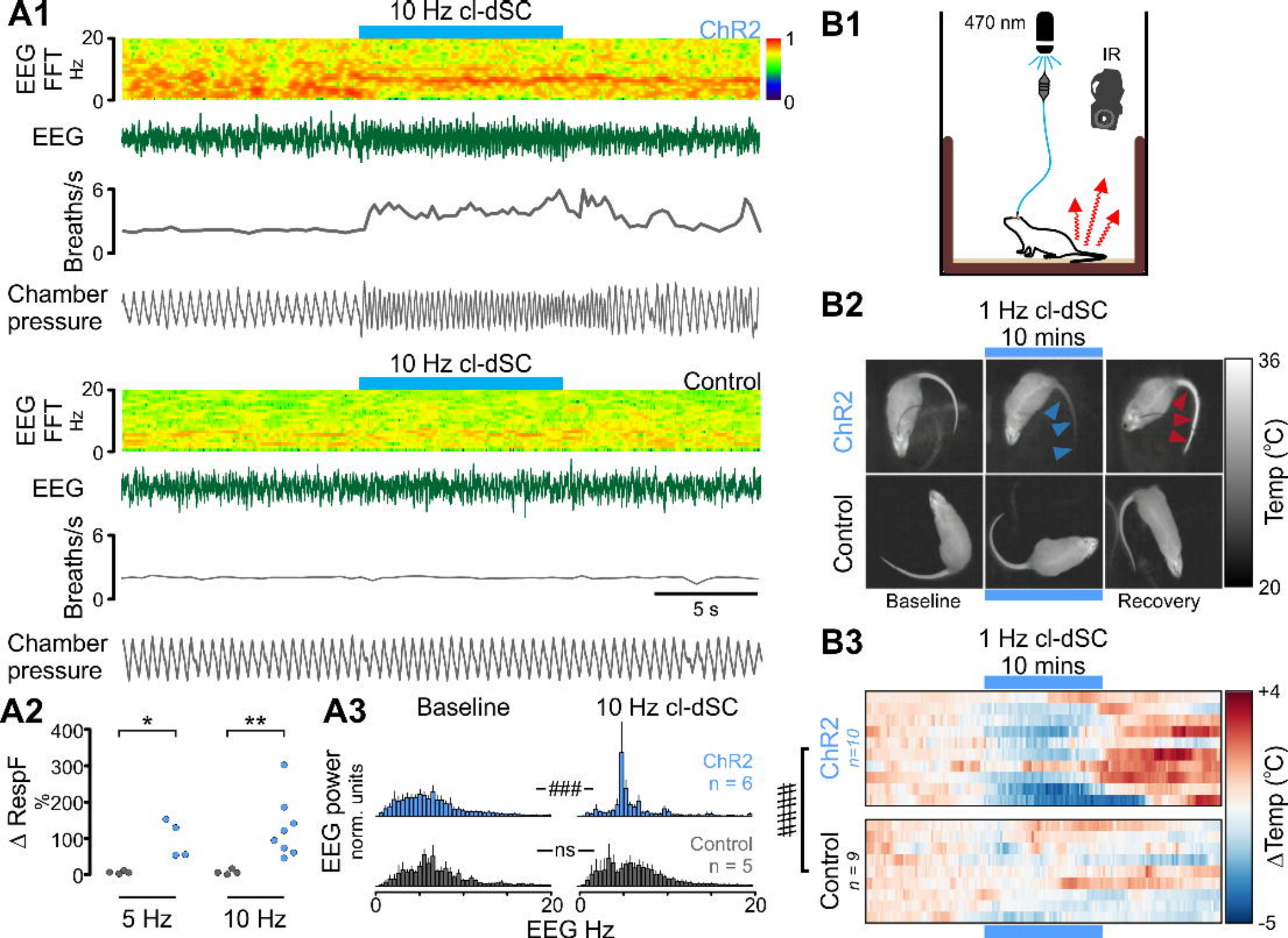
A1
10 Hz cl-dSC
ChR2
EEG FFT
Hz
20
0
1
0
EEG
Breaths/s
6
0
Chamber pressure
10 Hz cl-dSC
Control
EEG FFT
Hz
20
0
EEG
Breaths/s
6
0
5 s
Chamber pressure
A2
Δ RespF %
400
300
200
100
0
*
**
5 Hz
10 Hz
A3
Baseline
10 Hz cl-dSC
EEG power norm. units
ChR2
n = 6
Control
n = 5
–###–
–ns–
0
20
0
20
EEG Hz
B1
470 nm
IR
B2
1 Hz cl-dSC
10 mins
ChR2
Control
Baseline
Recovery
36
20
Temp (°C)
B3
1 Hz cl-dSC
10 mins
ChR2
n=10
Control
n = 9
+4
-5
ΔTemp (°C)

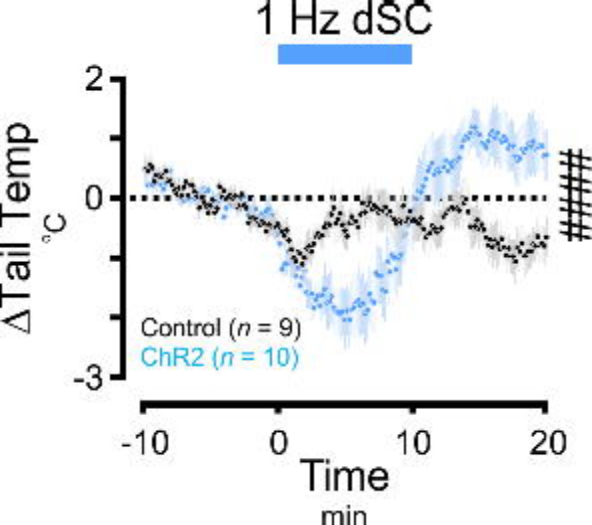
1 Hz dSC
2
0
-3
ΔTail Temp
°C
Control (n = 9)
ChR2 (n = 10)
-10
0
10
20
Time
min

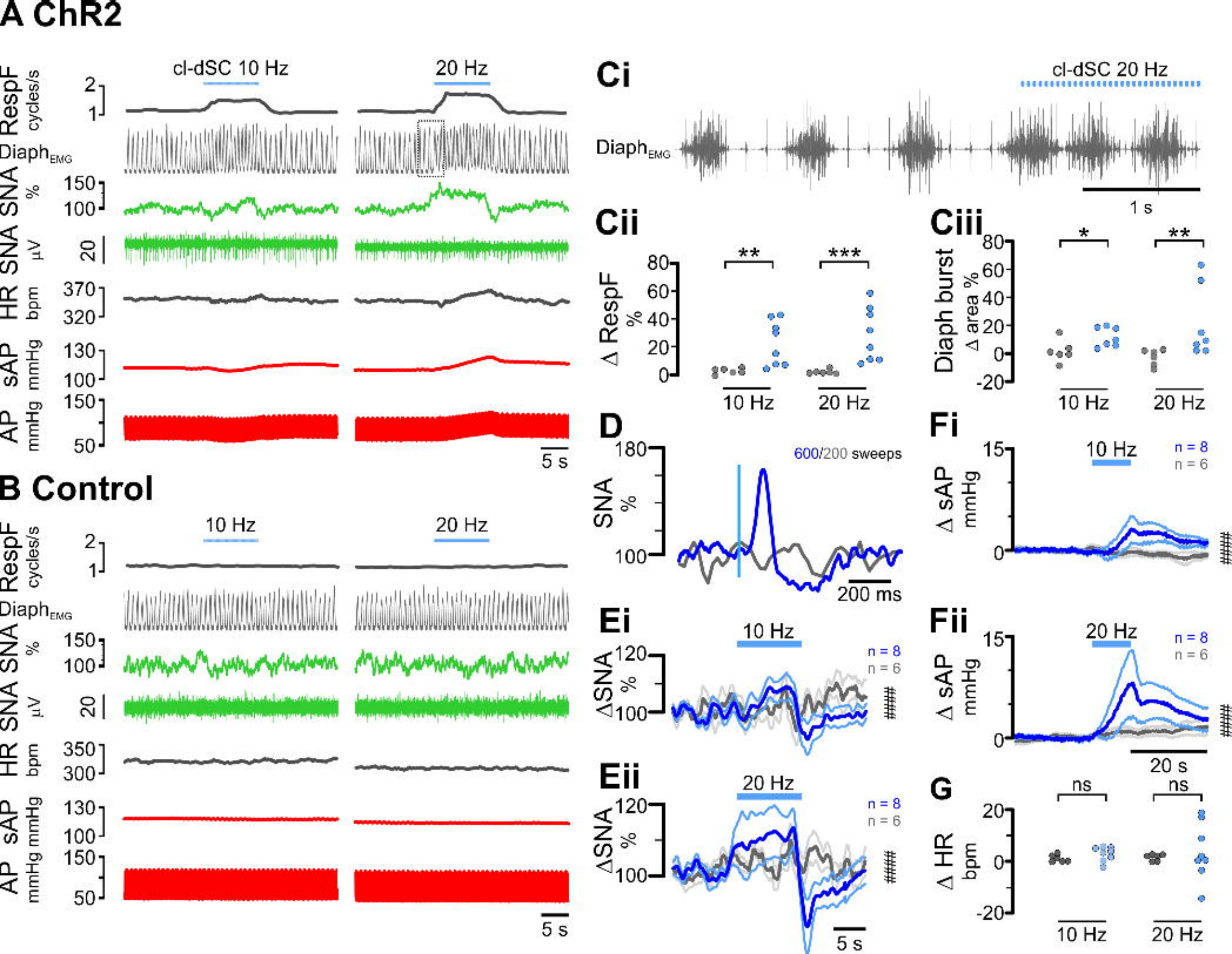
A ChR2
cl-dSC 10 Hz
20 Hz
RespF cycles/s
Diaph EMG
SNA %
SNA µV
HR bpm
sAP mmHg
AP mmHg
5 s
B Control
10 Hz
20 Hz
Ci
cl-dSC 20 Hz
Diaph EMG
1 s
Cii
Δ RespF %
10 Hz
20 Hz
Ciii
Diaph burst Δ area %
D
SNA %
600/200 sweeps
200 ms
Fi
Δ sAP mmHg
n = 8
n = 6
Ei
ΔSNA %
Fii
20 s
Eii
G
Δ HR bpm
ns

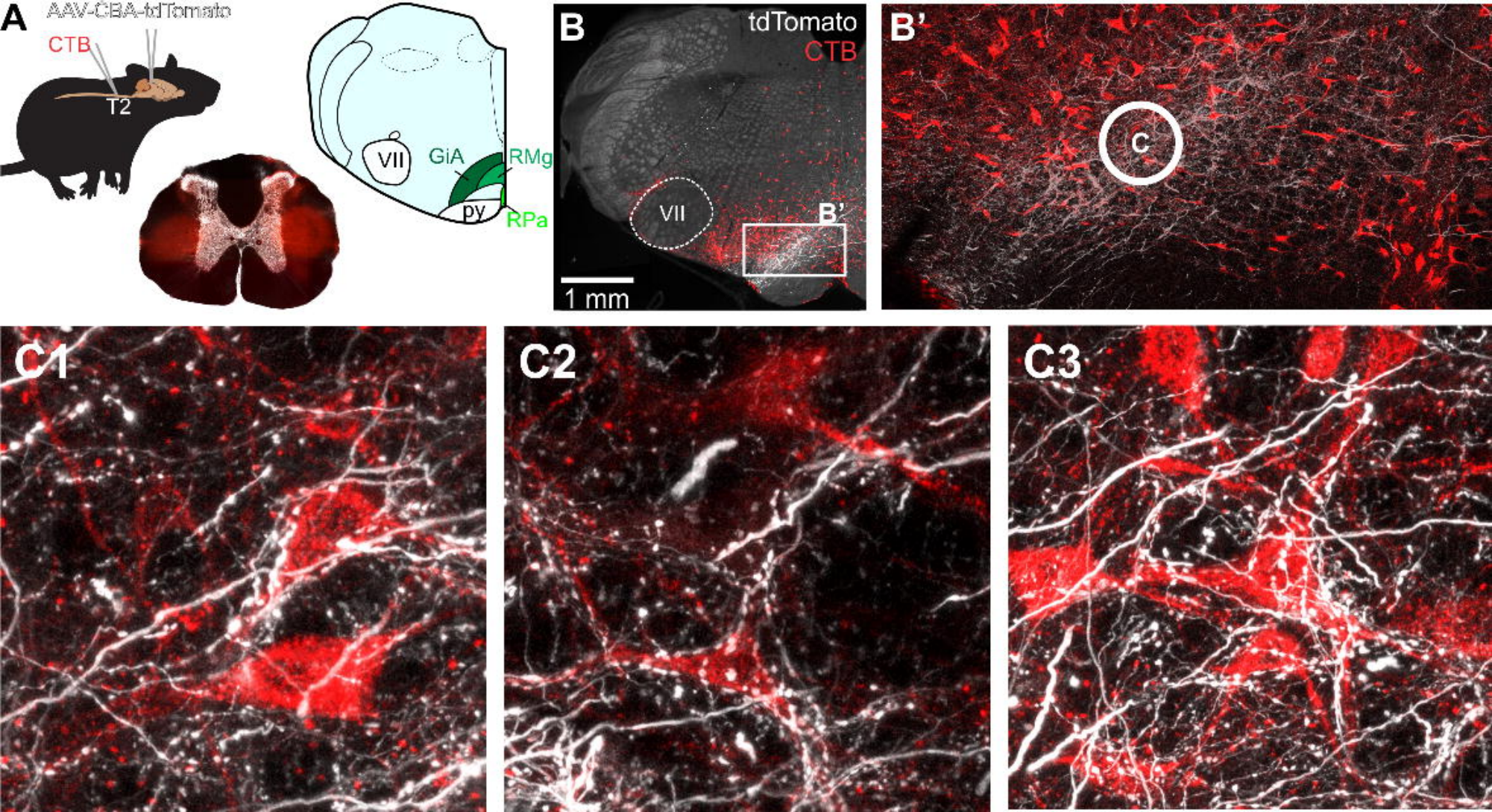
A
AAV-CBA-tdTomato
CTB
T2
VII
GiA
RMg
py
RPa
B
tdTomato
CTB
VII
B'
1 mm
B'
C
C1
C2
C3

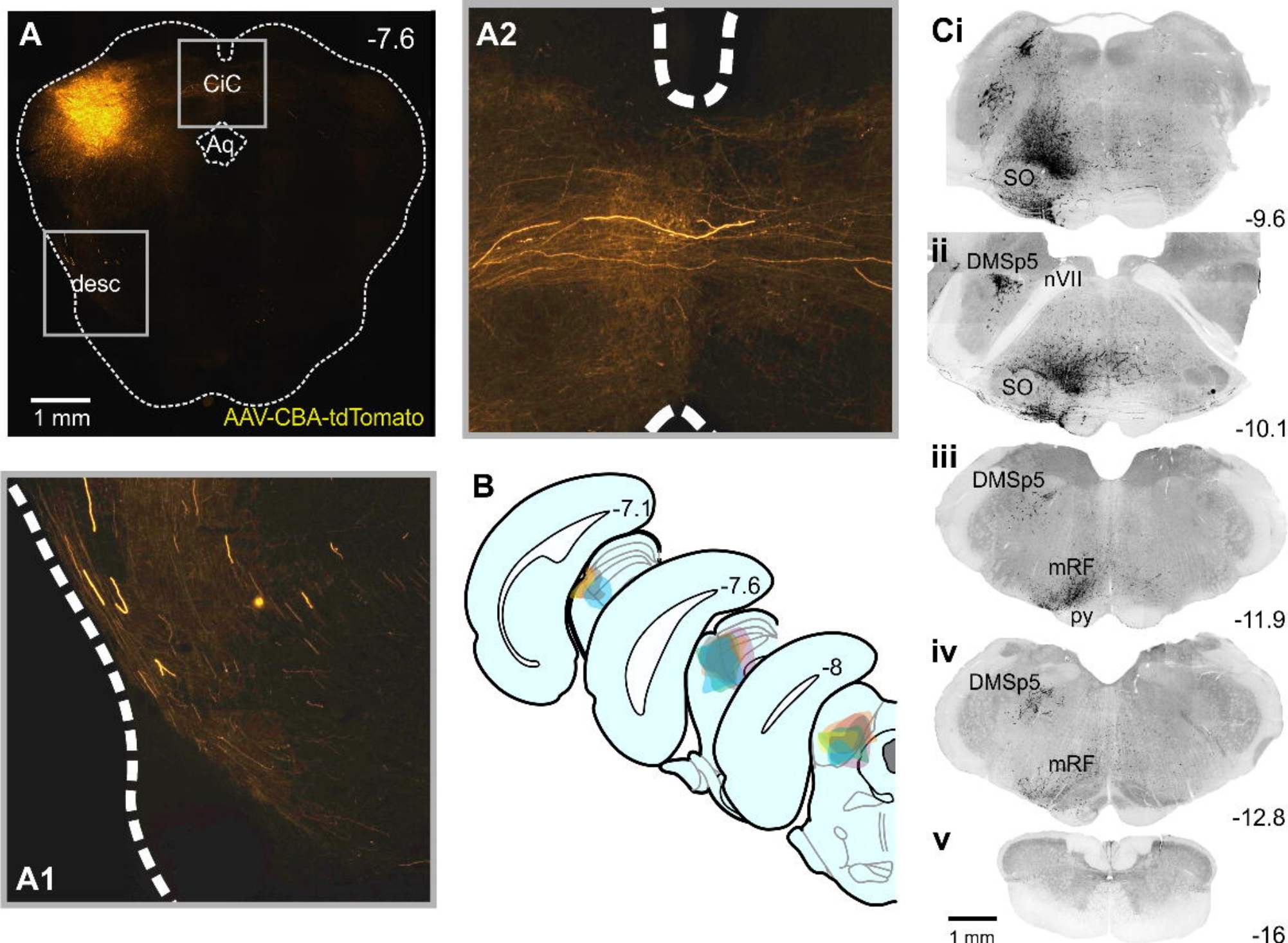
A
-7.6
CiC
Aq
desc
1 mm
AAV-CBA-tdTomato
A2
A1
B
-7.1
-7.6
-8
Ci
SO
-9.6
ii
DMSp5
nVII
SO
-10.1
iii
DMSp5
mRF
py
-11.9
iv
DMSp5
mRF
-12.8
v
1 mm
-16

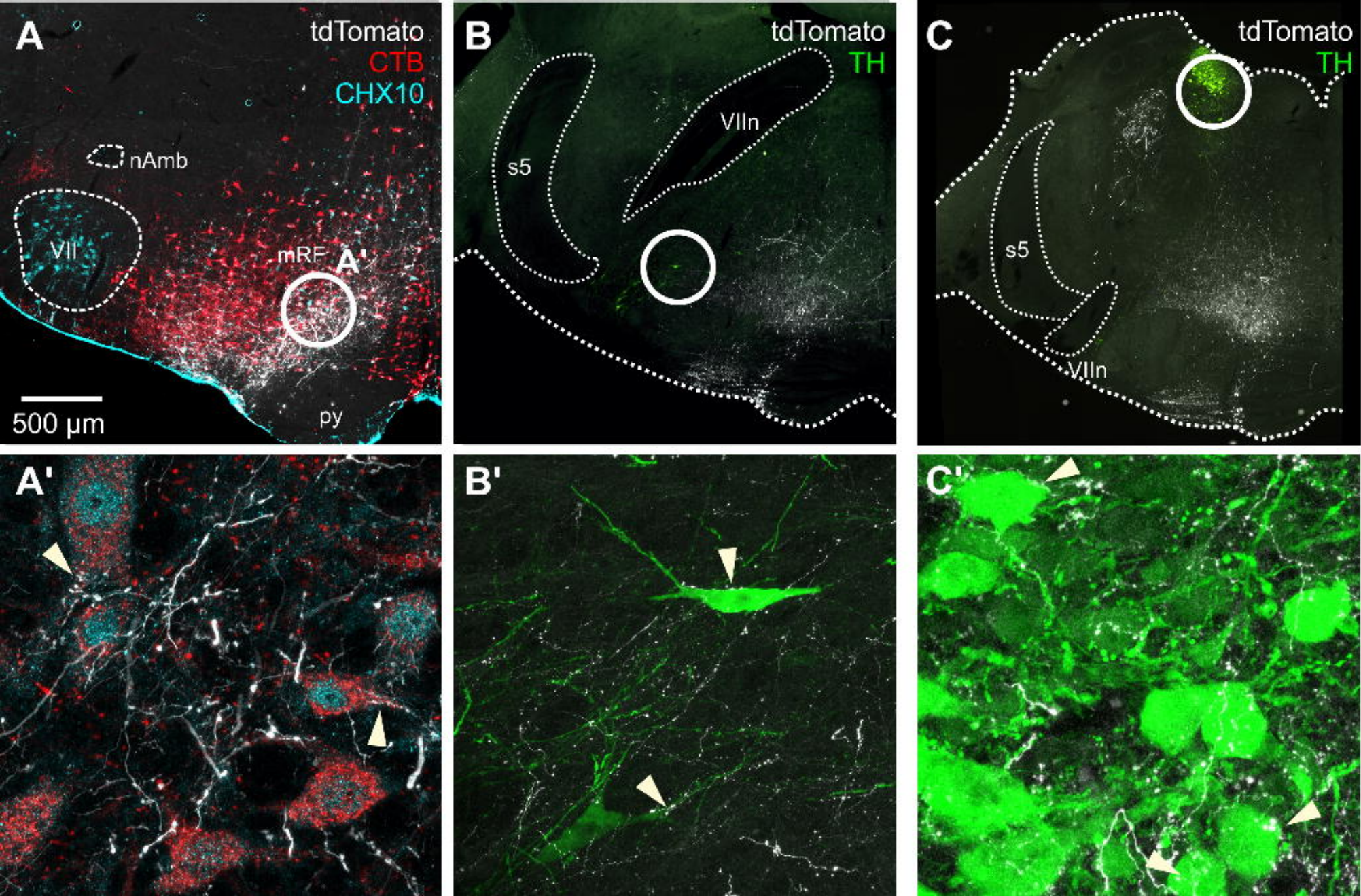
A
tdTomato
CTB
CHX10
nAmb
VII
mRF
A'
500 µm
py
B
tdTomato
TH
VIIn
s5
C
tdTomato
TH
s5
VIIn
A'
B'
C'

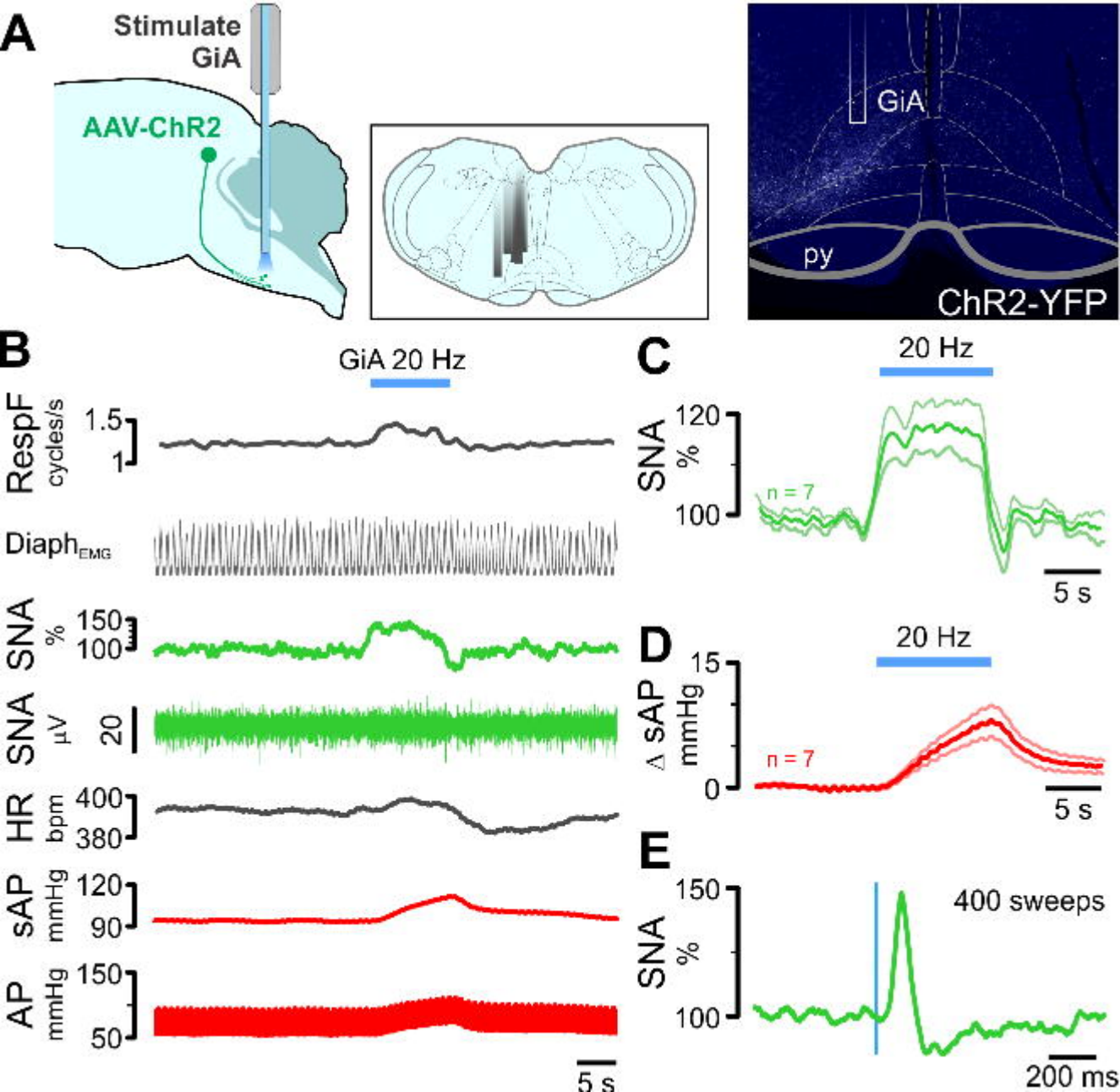
A
Stimulate GiA
AAV-ChR2
GiA
py
ChR2-YFP
B
GiA 20 Hz
RespF cycles/s
1.5
1
Diaph EMG
SNA %
150
100
SNA µV
20
HR bpm
400
380
sAP mmHg
120
90
AP mmHg
150
50
5 s
C
20 Hz
SNA %
120
100
n = 7
5 s
D
20 Hz
Δ sAP mmHg
15
0
n = 7
5 s
E
SNA %
150
100
400 sweeps
200 ms

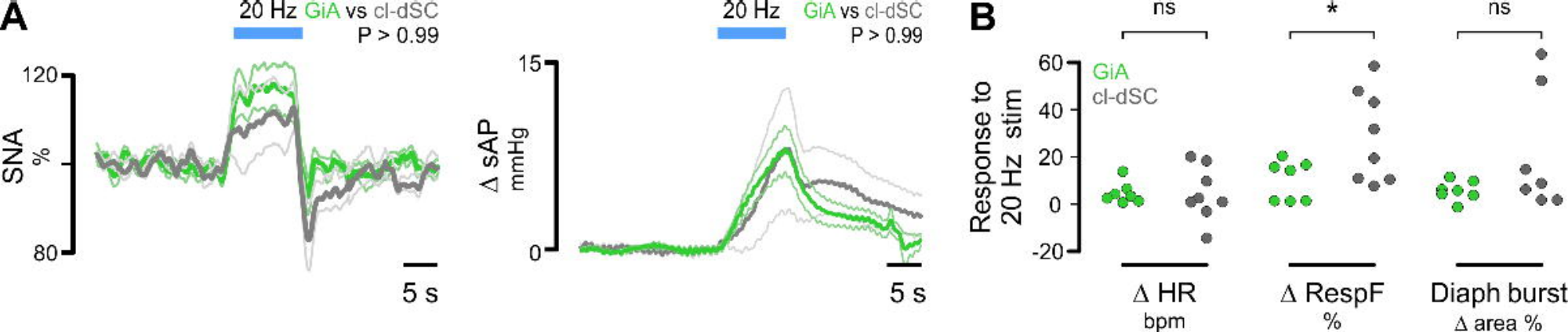
A
20 Hz GiA vs cl-dSC
P > 0.99
120
SNA
%
80
5 s
20 Hz GiA vs cl-dSC
P > 0.99
15
Δ sAP
mmHg
0
5 s
B
ns
*
ns
60
40
20
0
-20
GiA
cl-dSC
Response to
20 Hz stim
Δ HR
bpm
Δ RespF
%
Diaph burst
Δ area %

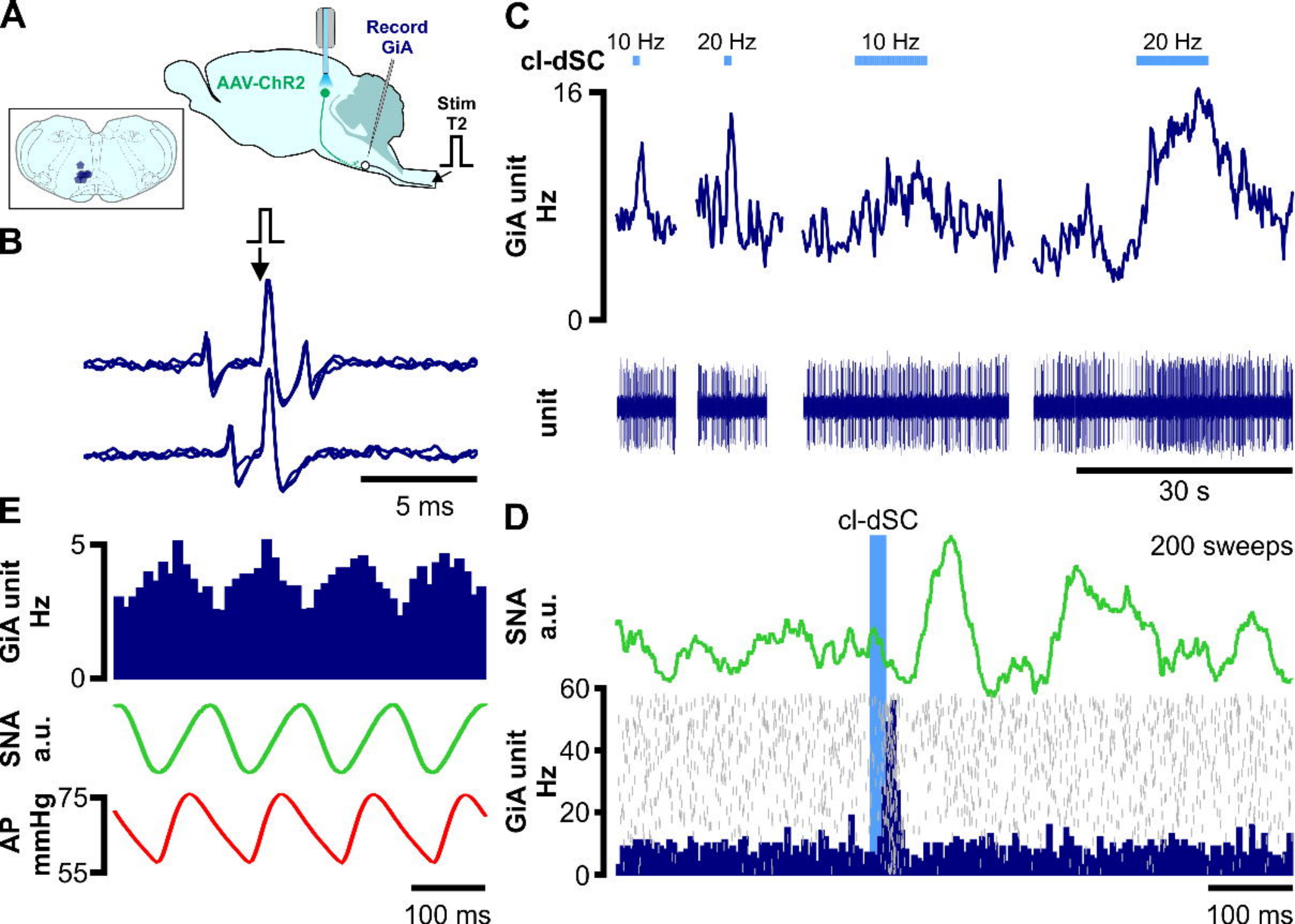
A
Record
GiA
AAV-ChR2
Stim
T2
B
5 ms
C
cl-dSC
10 Hz
20 Hz
10 Hz
20 Hz
16
0
GiA unit
Hz
unit
30 s
D
cl-dSC
200 sweeps
SNA
a.u.
60
40
20
0
GiA unit
Hz
100 ms
E
5
0
GiA unit
Hz
SNA
a.u.
75
55
AP
mmHg
100 ms